LIU-IEI-TEK-A--08/00442--SE

The Influence of Under Sleeper Pads on Railway Track Dynamics

Stephen Witt

2008-06-16

Supervisior:
Prof. Tore Dahlberg

Linköping University
INSTITUTE OF TECHNOLOGY

Department of Management and Engineering
Division of Solid Mechanics
SE-581 83 Linköping
Sweden

Abstract

In this work the influence of Under Sleeper Pads on the dynamic forces on a railway track is investigated. A special interest is devoted to the effect of using Under Sleeper Pads in a railway track with changing vertical stiffness. The contact force between wheel and rail and the ballast contact forces are examined. For the investigation a finite element model with the length of thirty sleepers is created and calculations are performed with the software LS-DYNA. Three different cases of varying vertical track stiffness are studied: the transition from an embankment to a bridge, a randomly varying track stiffness along the railway track and hanging sleepers.

Zusammenfassung

In der vorliegenden Arbeit wird der Einfluss von besohltern Schwellen auf die dynamischen Kräfte an einer Bahnstrecke untersucht. Besonders betrachtet wird der Effekt von besohlten Schwellen bei einer Bahnstrecke mit wechselnder vertikaler Steifigkeit. Dabei werden die Kontaktkraft zwischen Rad und Gleis sowie die Kontakkräfte am Schotterbett betrachtet. Für die Untersuchung wird ein Finite Elemente Model mit einer Länge von dreißig Schwellen erstellt und Berechnungen werden mit der Software LS-DYNA durchgeführt. Drei verschiedene Fälle von varieriender Streckensteifigkeit werden betrachtet: der Übergang zwischen einem Bahndamm und einer Brücke, eine zufällig streuende vertikale Steifigkeit entlang der Bahnlinie und hängende Schwellen.

Contents

List of Figures

List of Tables

1 Introduction

In recent years more and more high speed tracks, with train speeds over 200 km/h, have been built. Also the weight per axle of the trains has increased in the past. Both effects, i.e. higher speed and higher axle load, lead to higher stresses in the railway track when the track is loaded by the passing trains. The higher stresses speeds up the track deterioration. As a result the maintenance costs of high speed tracks increase considerably as compared to low speed tracks for trains with speeds less than 200 km/h.

To keep the track deterioration (for example track settlement) and the maintenance costs low, a well chosen vertical track stiffness is needed. But many railway tracks are very old and they were built without considering the soil stiffness. Therefore the tracks are often built on a very soft soil. Also, the soil stiffness varies along a railway track. This leads to a varying vertical stiffness of the whole track. Elements of the track, like turnouts, hanging sleepers, embankments or bridges, influence the vertical track stiffness of the railway track as well. A changing vertical track stiffness causes higher contact forces between the wheels and the rails. Also vibrations are caused. As a result of this the track deterioration rate speeds up. To modify the vertical track stiffness Under Sleeper Pads (USPs) may be used. These are elastic pads which are placed between the sleepers and the ballast. USPs are expected to reduce the influence of varying track stiffness on the wheel/rail contact force and to distribute the load of the train to a larger ballast area.

In this work the influence of using USPs on the wheel/rail contact force and on the ballast contact force is examined. Therefore three different cases of varying vertical track stiffness are studied: The first one is the transition between two areas with constant, but different, stiffnesses. An example of such a transition area is experienced by a train moving from an embankment to a bridge. The second case is a track with a randomly varying vertical stiffness along length. The last case studied is hanging sleepers. Hanging sleepers have no contact with the ballast bed and therefore the track becomes softer at this place. For all three cases studied the contact forces are calculated and evaluated.

2 The railway track

The requirement for the railway track is to guide the train. This should occur in a safe and economic way. For achieving these requirements the railway track must have a constant level and a perfect alignment. If these requirements are not fulfilled, the train will perceive many irregularities while moving along the track; one example is the joint of two rails. These irregularities will cause vibrations of the train, and this leads to discomfort for the passengers. Also, these vibrations may be hazardous to sensitive goods transported by the train. Furthermore, the noise caused by the passing train should be low. Otherwise passengers and people staying near the railway track get disturbed.

The railway track is loaded with the weight of the train. This load should be transmitted to a large area in order to reduce the stress in the substructure. By the rail and the sleepers the wheel/rail contact force is transmitted from a small area of a few square centimeters to an area of up to one square meter in the subgrade.

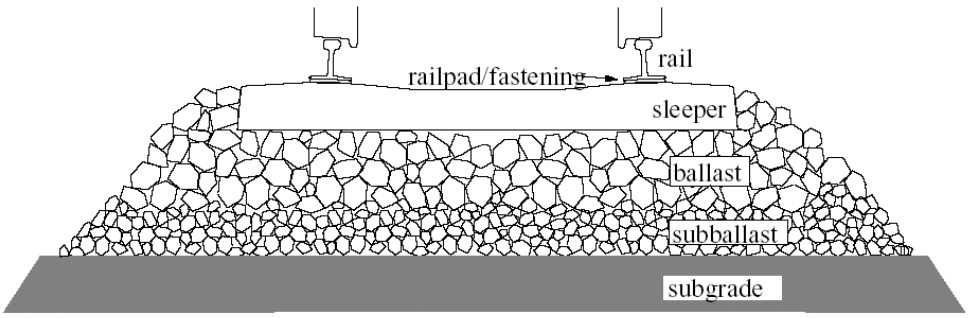

Figure 2.1: Construction of a modern railway track

Figure 2.1, taken from Dahlberg [2], shows the construction of a modern railway track. Nowadays a railway track consists of several components: rails, railpads, fastenings, sleepers, ballast, subballast and subgrade. This track construction is divided into two main parts: the superstructure and the substructure. The components counted to

these two parts differ between several authors. All of them consider the rails, sleepers, railpads and fastenings as parts of the superstructure and the subgrade - as a formation layer - and the ground as parts of the substructure. Differences exist in the classification of the ballast. While for example Remennikov and Kaewunruen [17] count the ballast as a part of the substructure, Dahlberg [2] describes the ballast as a part of the superstructure.

The rail consists of steel and has a design similar to an I-profile. In modern track the most commonly used rail profile is the UIC60 rail. The sixty indicates that one meter of this rail profile has a mass of 60 kg. The head of the rail is treated in order to improve the friction resistance. The surface of the rail should allow a smooth running of the wheelsets. The load of the passing trains must be carried by the rails. These transmit the load of the trains to the lower components of the railway track. Lateral and longitudinal forces should also be carried by the rail and be transmitted to the lower laying components.

The sleepers distribute the load of the train, which is transmitted by the rails, to the ballast. Another requirement for the sleepers is to fix the rails in their position. Thereby the track gauge, the track level and the alignment of the track are secured. The demands on the sleepers are dimensional accuracy, resistance to weathering and low costs of maintenance. The possible materials for sleepers are wood, steel and prestressed concrete. Sleepers of prestressed concrete have a higher weight and therefore a better position stability. Because of this and their long life-cycle of about 40 years mainly sleepers of prestressed concrete are used when building new tracks nowadays.

Between the rails and the concrete sleepers are elements known as railpads placed. The railpads protect the sleepers from crushes of the rail when a train is passing. Thereby the life-cycle of the sleepers gets increased. The railpads have an influence on the track stiffness. Soft railpads cause a larger deflection of the rail and the load of the train is transmitted to more sleepers. Also high frequency vibrations and their transmission to the sleepers and the ballast are suppressed by the softer railpads. Stiffer railpads produce a higher load on a single sleeper and let the high frequencies pass to the lower part of the railway track. But the deflections of the rails are less than when using soft railpads.

The rails are fixed to the sleepers by special fastenings. These fastenings provide a displacement of the rails and the sleepers. In most simulations the fastenings are not included, because their stiffness is much lower than the stiffness of the railpads. Nevertheless, the fastenings will create a static preload on the railpads.

The sleepers are embedded in the ballast bed. The ballast layer prevents a displacement of the sleepers and the rails. Furthermore the ballast layer has to carry the forces from the train. These are distributed over a large-sized area to minimize the stress in the subgrade. The ballast layer consists of coarse stones, which are highly compacted to avoid track settlement and to keep the track level constant. Normally the depth of the ballast bed is at least 0.3 m and the width is at least 0.5 m from the ends of the sleepers. The design of the ballast bed should facilitate drainage of water. If the water can not drain, plants will start to grow in the ballast bed. The structure of the ballast bed gets weakened by these foulings. Furthermore the stones used for the ballast bed must have a correct size. Stones which are too small prevent the water drainage, while too big stones give an uneven support of the track.

Between the ballast layer and the subgrade there is a special layer that prevents a mixing of these two layers. This subballast layer consists of smaller stones, such as sand or gravel materials. This layer also prevents damages caused by frost penetration. It is important that the subballast does not prevent the water that comes from the ballast to flow out from the track bed. Furthermore, the subballast decreases the appearance of plants which can grow from the ground into the ballast bed and weaken it.

The subgrade gives the surface on which the ballast bed is placed. It consists mostly of earth and rocks and it is leveled off for getting a constant height of the track. The subgrade is very important for the behavior of the track. For example the stiffness of the subgrade, and therefore of the whole railway track, can vary very much within a few meters. Unfortunately the subgrade can not be modified after the track has been laid and often it is also not part of the maintenance operations.

3 Track settlement

As mentioned in Chapter 2 a railway track is loaded by the passing trains. The load of the passing trains causes deformations of the ballast and the subground structure of the railway track. These deformations can be non-elastic. In this case the track does not go back to its original position after being unloaded. Thus the track gets a new position which is very close to the original one. When passed by many trains during the life-cycle of the railway track these single deformations add more and more. Thereby the deformations can differ in single parts of the track, so that irregularities in the track level are generated. This degradation of the track is known as differential track settlement [13]. The track settlement can be divided into two main phases.

The first phase of track settlement starts directly after building the track. Under the forces of the first passing trains the stones move into other positions so that the gaps between them become smaller. The second phase of track settlement starts after the first one has finished. This phase is determined by the behavior of the ballast and the subground. In this phase the track settlement is slower and more or less constant to the time and the load of the passing trains. A reason for track settlement in this phase is for example a volume reduction of the ballast material. The volume reduction is caused by an ongoing motion of the ballast stones whereas the gaps between the ballast stones get further reduced. Also the load of the trains can cause breakings or even pulverization of some stones [7]. In addition to the volume reduction the stones move under the load of the trains. This motion can cause abrasive wear on the contact areas of single stones. Thereby the stones get a rounder form and require less space. Another reason for the track settlement in the second phase is the movement of the sleepers under the forces of the train. By the moving sleepers stones are pushed away and the sleepers sink deeper into the ballast bed. But there is also an opposite effect possible. The load of the train is transmitted by the wheels to the rails and causes a bending of these. As a consequence of this the sleepers are lifted by the bending rails in front of and behind the wheels. Stones can fall into the generated gaps between the sleepers and the ballast. After unloading the railway track the gaps get closed and the rail track has got a higher level at these parts.

The track settlement leads to a track with different levels of height. These different track levels cause irregularities that will increase the wheel/rail contact force. Consequently a passing train induces more damage to the railway track and causes an increased degradation of the railway track. This again leads to a progress of track settlement. Therefore, when the track settlement once has started it will be very difficult to stop it.

4 Under Sleeper Pads

USPs are special pads which are placed between the sleepers and the ballast. They are about 10 mm to 20 mm thick and have been used for about 20 years in special applications. In recent years the use of USPs has increased, mainly in newly built high speed railway tracks in Central Europe. According to Johansson [8], the USPs often consist of a polyurethane elastomeric material which has a foam structure. Often the USPs consist of two materials, whereby an outer material protects an inner material from abrasive wear. The materials must be well chosen in order to get good damping and stiffness values. For the installation in the railway track, the USPs are often glued onto the underside surface of the sleepers.

The main reason for using USPs is to reduce the damage of the ballast. A soft USP fits better with the stones, which can be pressed into the soft pad. Thereby the contact areas of the force-carrying stones get increased. According to Riessberger [18] normally only 3 to 4 % of the sleeper's area is in contact to stones. When using USPs the contact area incresaes to nearly 30 % of the sleeper's area. This leads to a reduced contact pressure. Also the abrasive wear of the stones is expected to become less. By using USPs the force of the train is expected to be distributed to more sleepers at the same time. This also reduces the contact pressure and the wear of the ballast and therefore the track settlement. Furthermore it is expected that vibrations in the ballast and in the ground are reduced by using USPs.

The vertical stiffness of a railway track can change very rapidly within a few meters. The railway track is seldom build on a homogeneous subground. Therefore the subground changes its properties, including its stiffness, along the track. The change of track stiffness is more or less random. The result of a track stiffness measurement done by Banverket with a measurement vehicle [1, 13] is shown in Figure 4.1. By using USPs the variations of stiffness along the track can be compensated. These smoother stiffness variations lead to less maintenance work on the railway track. Also vibrations can occur at areas with a sudden change of the railway stiffness like for example at transition areas from an embankment to a bridge or at crossovers and switches. With USPs these changes of stiffness can be made smoother and thereby the vibrations get

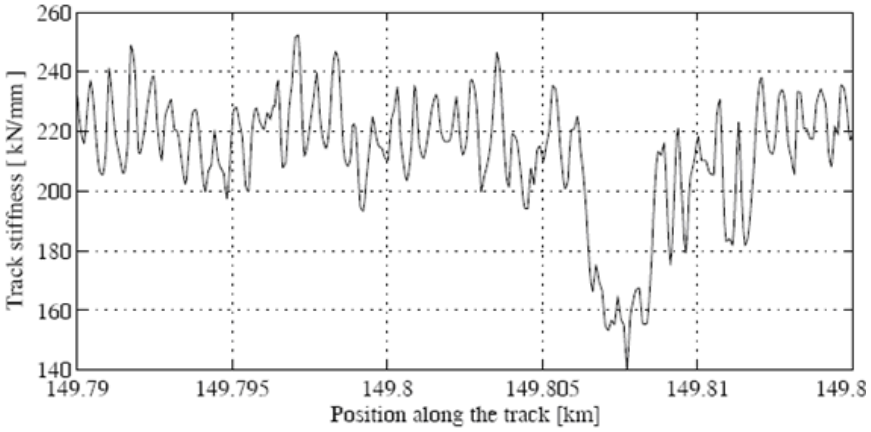

Figure 4.1: Track stiffness measurement done by Banverket

reduced. Moreover, according to Riessberger [18] is it possible to reduce the thickness of the ballast layer when building a railway track with USPs.

The requirements for USPs are resistance against abrasive wear by the stones, especially against the sharp corners of the stones. Therefore, as mentioned above, a special outer layer is often used. The USPs must also permanently withstand the loadings of the passing trains without loosing their elastic properties. The vibration behavior of the USPs should also fit with the requirements for the track. Furthermore, the installation of the USPs and track maintenance should be possible in an easy way without requiring new machines that cause additional costs.

5 The computer model

In this work a finite element model is used which consists mostly of 3D solid elements. In order to keep the calculation time short only one half of a railway track is modeled and symmetry with respect to the centre line is assumed. The model consists of a rail, a wheel, railpads, sleepers, USPs and the ballast. In the following sections the model is described in more details.

5.1 Solution methods

Train/track interaction computational models can be solved in two ways: by frequency-domain method and by time-domain method. In the following section both methods are shortly described.

5.1.1 Frequency-domain method

With the frequency-domain method only fully linear systems can be treated. For solving such problems one must know the track receptance. An example of a track receptance, taken from Dahlberg [2], is shown in Figure 5.1. Regarding a stationary

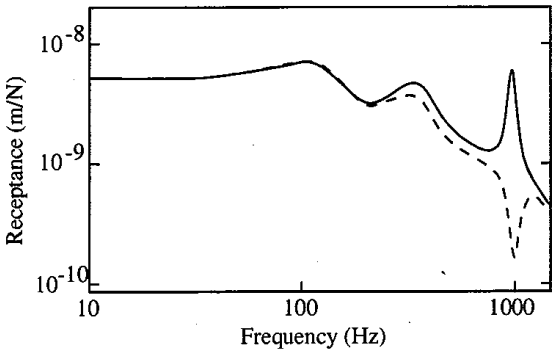

Figure 5.1: Track receptance

problem only the receptance of a point of the track is required. There are two opportunities to get the receptance of the track: the first one is to measure on a real track and the second one is to calculate it by using a track model. When investigating dynamic problems the wheel and the rail are excited at the contact patch with a prescribed displacement [2, 15]. To simulate a moving wheel, a strip with irregularities is pulled through the contact area. It is only possible to work with a stationary track response. Therefore singular events on the track, like for example varying track stiffness, hanging sleepers and rail joints, can not be simulated with the frequency-domain model.

5.1.2 Time-domain method

In the time-domain method the interaction forces and the displacements are calculated numerically by time integration. Hereby the wheel moves over the track with a predefined speed. Using this method the deformations of the wheel/rail contact area can be examined. Often the train is modeled as a rigid wheel but it can also be modeled in a more detailed way to improve the wheel/rail contact forces. The upgrades of computers in recent years allow a more and more complex modeling of the railway track and the train. The track is modeled with finite elements and can contain linear and non-linear components. Non-linear components can be, for example, the railpads and the ballast material. They have a big influence on the wheel/rail contact force. The model in this work is a time-domain model. It is therefore, for example, possible to simulate variations of track stiffness, hanging sleepers and loss of wheel/rail contact with this model.

5.2 Train model

The train model used in this work is kept simple. The train is simulated by just one wheel which is assumed to be a rigid body. Therefore the wheel is not modeled as a full circle filled with elements but only as a semicircle of shell elements with a radius of 500 mm. In this way the calculation time is reduced without influencing the results. The wheel in this simulation has a mass of 750 kg, simulating the mass of half a wheelset. The load of the train on half a wheelset is assumed to be 10,000 kg. Thus, the total static force from the train to one half of the track amounts to 107.5 kN. The material of the wheel is steel with a mass density of 7,800 kg/m^3. The Young's modulus is 210,000 MPa and the Poisson's ratio is 0.3. Both values are used for contact calculations. The wheel remains for 0.06 s in its staring position after the mass of the

wheel is loaded. After 0.06 s the waves induced by the mass loading have disappeared and do not affect the results anymore. Afterwards the wheel starts to move along the rail. The speed of the wheel used in the calculation is 90 m/s. A lower speed can be used but it would increase the calculation time of the computer.

5.3 Track model

The modeled track consists of the rail, railpads, sleepers, USPs and the ballast. The total length of the model is 30 sleepers, whereas the centre-to-centre distance between two sleepers is 600 mm.

The rail is modeled with an isotropic elastic material and has a rectangular cross section. Thus, it is not modeled as an I-profile, but the cross section is selected in such a way that it has the same properties as the original rail profile. By not using an I-profile for the rail less elements are required in the model and the computation time is decreased. The width w of the rail profile is 50 mm, the height h is 194 mm. It has a mass density ρ of 6,186 kg/m^3. Therefore the mass m of one meter of the rail is

$$m = w \cdot h \cdot \rho = 60.0 \, \frac{kg}{m}. \tag{5.1}$$

This represents an UIC 60 rail, which is used in most newly built tracks in Europe nowadays. The Young's modulus of the rail is 210,000 MPa and the Poisson's ratio is 0.3. The overall length of the rail is 18.1 m.

The railpads are modeled with a hyperelastic rubber, which is nearly incompressible. The railpads are placed over the full width of the sleeper and are 50 mm wide. Their height is 10 mm. The chosen shear modulus of the railpads is 50 MPa. The Young's modulus of the material can be calculated by

$$E = \frac{G}{2 \cdot (1 + \nu)} \tag{5.2}$$

The Poisson's ratio ν of the material is 0.463. The stiffness of the railpads is 146 kN/mm. A preload because of the fastenings is not included in this model.

The railpads are placed between the rail and the sleepers. In this model concrete sleepers are used. They are modeled with rectangular cross section. The height and the width of the sleepers are 200 mm each. The length of a full sleeper is 2.5 m. With a mass density of 2,500 kg/m^3 half a sleeper, like the one used in this model, has a mass of 125 kg. Like the wheel also the sleepers are considered rigid. Therefore, bending of

the sleepers are not simulated by this model. This implies that the computation time is reduced.

The USPs used in this study are modeled with an isotropic elastic material. They cover the same area as the sleepers and they are 20 mm thick. Their mass density is 500 kg/m^3 and their Poisson's ratio is 0.1. The Young's modulus of the USPs is changed between different calculations in order to change the stiffness of the USPs.

Like the rail and the USPs the ballast is also modeled with an isotropic elastic material. The upper area on which the sleepers are placed has a width of 1,500 mm and the width on the lower area on the soil is 2,500 mm. The height of the ballast is 1,000 mm. The mass density of the material used for the ballast is in this model 2,500 kg/m^3 and the Poisson's ratio is 0.1 like for the USPs material. In order to simulate a stiffer and a softer track the Young's modulus of the ballast material is changed.

To avoid reflections on the boundaries of the model, non-reflecting boundary conditions are used. Thereby pressure and shear waves are absorbed at the boundaries, so that the results are not influenced by them.

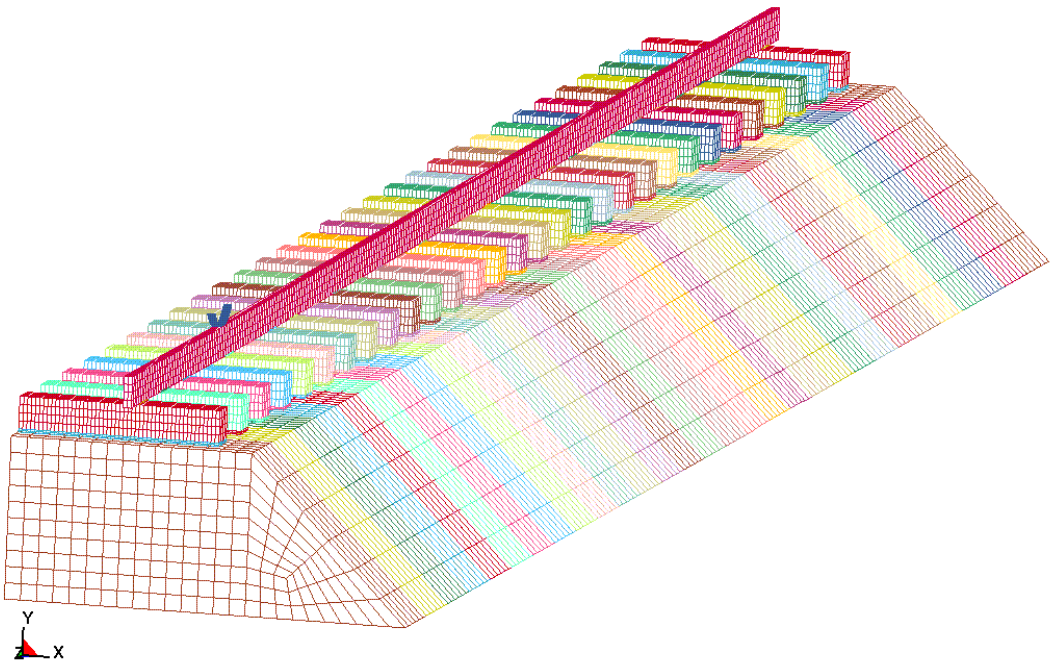

Figure 5.2: Picture of the used model

5.4 Programs used

The model used in this work is built with the preprocessor software *TrueGrid*. The calculations are done by using the finite element software *LS-DYNA*, which is able to solve dynamic non-linear problems. It works with an explicit solver and is much faster than an implicit solver [13]. In order to capture also high-frequency waves, *LS-DYNA* automatically sets the timestep small [5]. The timestep Δt is calculated with the following formula:

$$\Delta t = \frac{l_e}{c} \tag{5.3}$$

Here l_e is the length of the smallest element used in the model and c is the speed of sound. The speed of sound is calculated by

$$c = \sqrt{\frac{E}{\rho}} \tag{5.4}$$

In this formula E is the Young's modulus of any material used in the model and ρ is the corresponding mass density. Therefore the time needed for the calculation of one run - the wheel moves along the full rail length - depends on the chosen stiffness of the separate parts of the track model.

On a computer with a 1.9 GHz Pentium 4 processor and 1 GB Ram the calculation time is about twelve hours.

6 Methods of evaluation

In order to evaluate the received force-time diagrams of the wheel/rail contact forces and of the ballast contact forces two methods are used. In the first method the average value and the standard deviation of the force signals are calculated. In addition to this method load spectra are calculated with level-crossing counting in order to get a method to evaluate the oscillations. At both methods the signal is analyzed between the times of 0.08 s and 0.25 s. An analysis before 0.08 s is not useful, because vibrations which are generated at the beginning of the motion of the wheel at a stiff track have not faded away before this time. Therefore, the amplitudes could be very high and would lead to wrong conclusions. At the time of 0.25 s the wheel reaches the end of the rail and loses the contact to it. Consequently the wheel/rail force becomes zero afterwards. The mean $\overline{x}$ of the force is calculated with

$$\overline{x} = \frac{1}{n} \cdot \sum_{i=1}^{n} x_i \tag{6.1}$$

Here n is the number of values and x_i are the single values. The standard deviation s is calculated with the following formula:

$$s = \sqrt{\frac{1}{n-1} \cdot (\overline{x} - x_i)^2} \tag{6.2}$$

The method of level-crossing counting extracts a collective out of a signal over time. Thereby a collective is characterized by its maximum amplitude, its occurrence and its form. In the level-crossing method the ordinate of the time signal is divided into several levels. Afterwards the times each level is crossed by the signal are counted. Hereby one counts either the up-crossings or the down-crossings of the time signal. With this method the maximum and minimum values of the time signal are recorded. But the amplitudes and the means of the single cycles are not recorded. According to Haibach [4] a damage analysis with a collective extracted by the level-crossing method is not useful. However a level-crossing load spectrum gives a good overview of a time signal by showing the maximum and minimum values and the form of the time signal. Furthermore, if one level is crossed by every single cycle, then the load spectrum will give the number of cycles of the time signal.

7 Transition area

7.1 Explanation

As mentioned before the vertical track stiffness changes along the track. A large change of the vertical stiffness of a railway track occurs when the train reaches a bridge or an embankment. In theses cases the track stiffness changes rapidly within only a few meters. Figure 7.1 shows the result of a measurement performed by Banverket. The measurement was done on the west coast line in Sweden in 2001 with a measurement trolley as described by Berggren [1]. The figure shows the change of vertical stiffness on a bridge at 9.4 km and at an embankment from 11.4 km to 11.7 km. The figure is taken from Dahlberg [2] and shows that the track becomes stiffer on a bridge and softer on an embankment. The stiffness changes in this case with a factor higher than two.

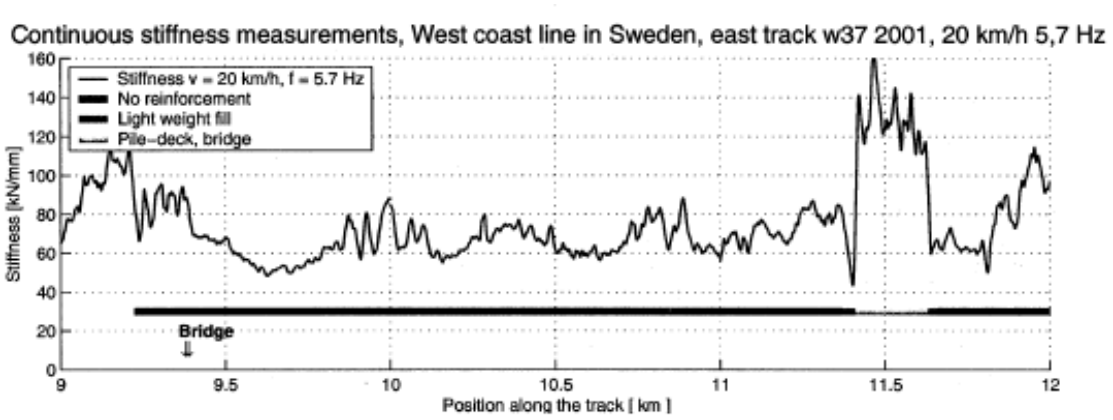

Figure 7.1: Vertical stiffness along a railway track

The change of stiffness at the embankment is almost four, from about 40 kN/mm at km 11.40 to 160 kN/mm at km 11.45.

In this chapter such a rapid change of vertical stiffness is simulated. Therefore the Young's modulus of the ballast is changed. The thirty sections of the model are separated into two parts. The first part contains fourteen sleepers and the second one sixteen sleepers. In the first part the ballast has a Young's modulus of 30 MPa. In the

second part the Young's modulus of the ballast is set to 110 MPa. With the Young's moduli chosen the stiffness of the ballast is 20 kN/mm in the soft section and 60 kN/mm in the stiff section. Thereby a transition from a soft to a stiff area is simulated. According to Lundqvist [13] this case is worse than a transition from a stiff to a soft area.

Four different cases are studied. In the first case the model is solved without using any USPs. Afterwards three different types of USPs - stiff, medium and soft - are used. The values of the three used types of USPs are shown in Table 7.1.

USPs	**Young's modulus**	**vertical stiffness**
stiff	1000 MPa	3000 kN/mm
medium	100 MPa	400 kN/mm
soft	10 MPa	50 kN/mm

Table 7.1: The three types of USPs used

7.2 Calculations

7.2.1 Wheel/rail contact force

The wheel/rail contact forces for all four cases are shown in the Figures 7.2 to 7.5. The forces are examined only in the time between 0.08 s and 0.25 s as mentioned in Chapter 6.

The wheel/rail contact force without using USPs (Figure 7.2) increases when the rail passes the transition area at 0.158 s. In the soft part (to the left in the figure) the contact force oscillates. In front of the transition the contact force increases and a peak occurs and afterwards a trough. The range of the load change is 35 kN. Afterwards the contact force oscillates again, but with higher ranges than in the soft part.

The contact force for using stiff USPs (Figure 7.3) looks quite similar to the curve without USPs. There is also a peak and a trough at the transition zone with a range of 35 kN. Also the oscillation at the stiff part increases.

When using medium USPs (Figure 7.4) the oscillation in the first part of the track has a longer period than without using USPs. The peak at the transition area still exists, but it becomes smaller. In this case the range is now only 24 kN. Afterwards, again the oscillation on the stiff part has a longer period but also a higher range.

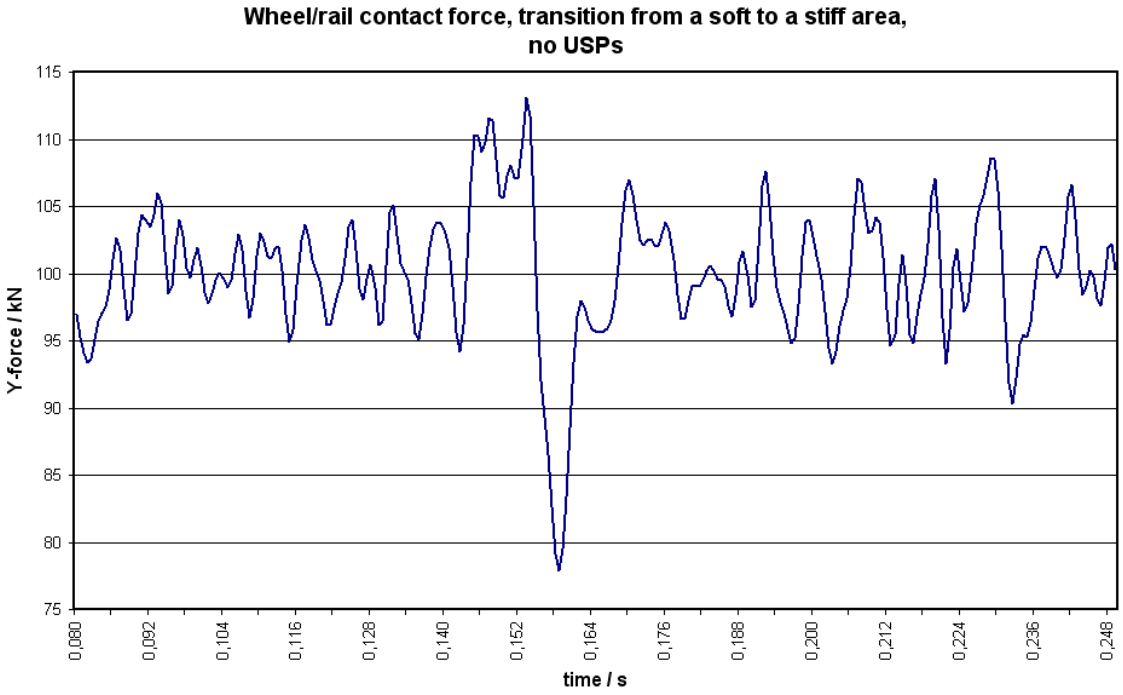

Figure 7.2: Vertical wheel/rail contact force with no USPs at a transition

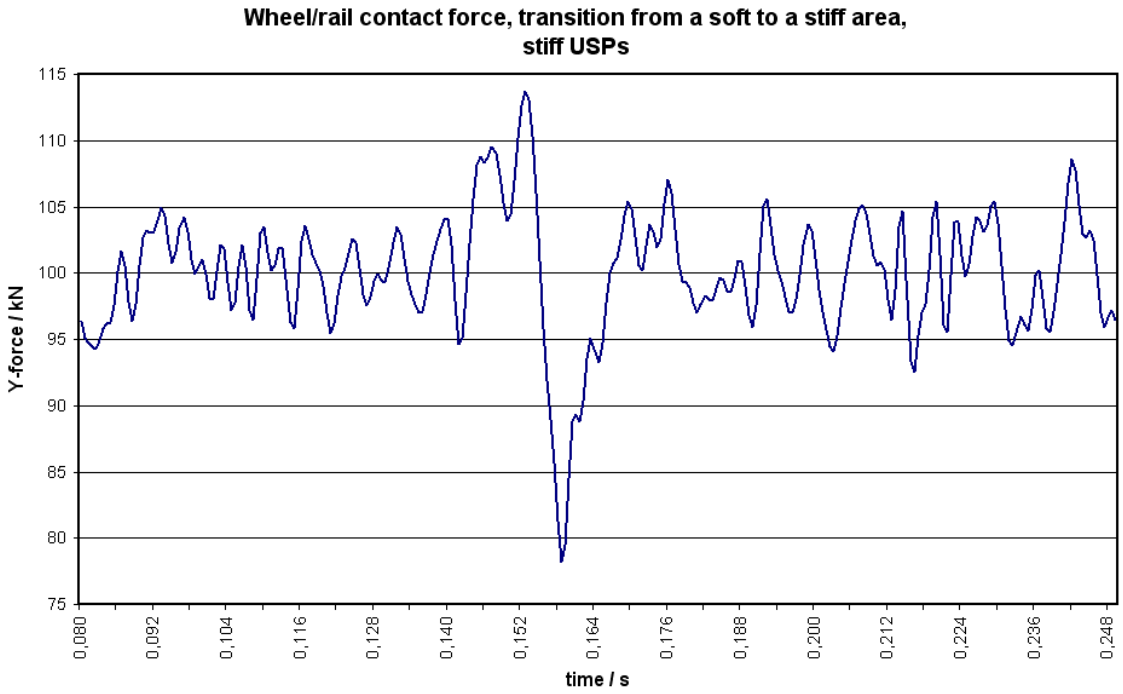

Figure 7.3: Vertical wheel/rail contact force with stiff USPs at a transition

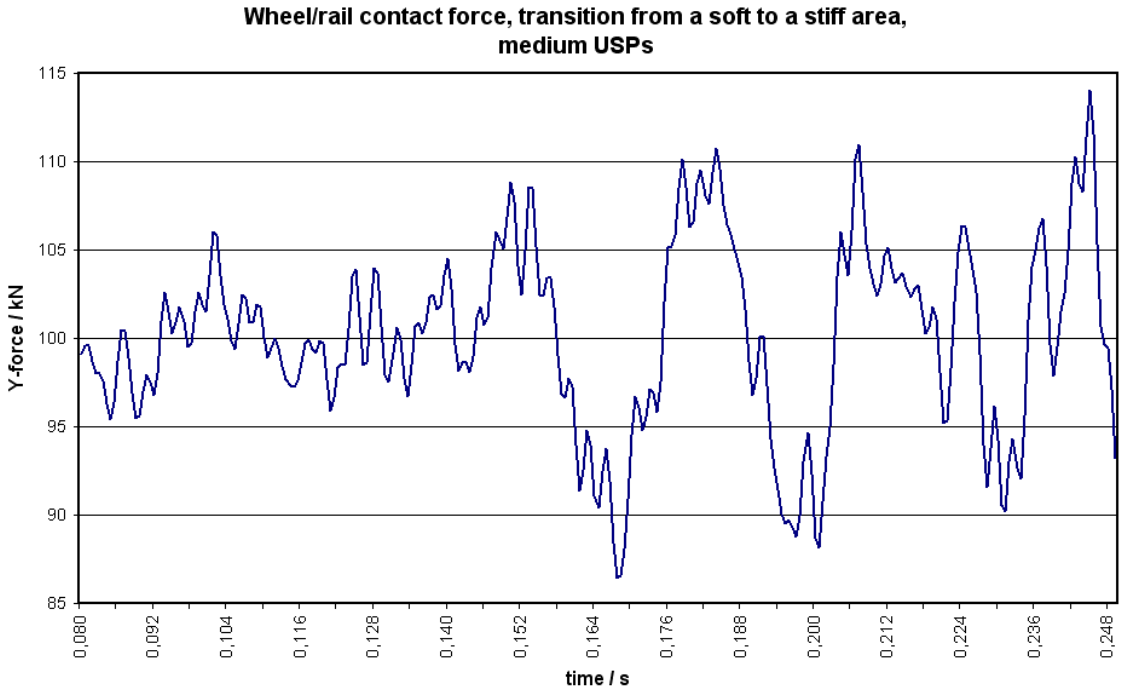

Figure 7.4: Vertical wheel/rail contact force with medium USPs at a transition

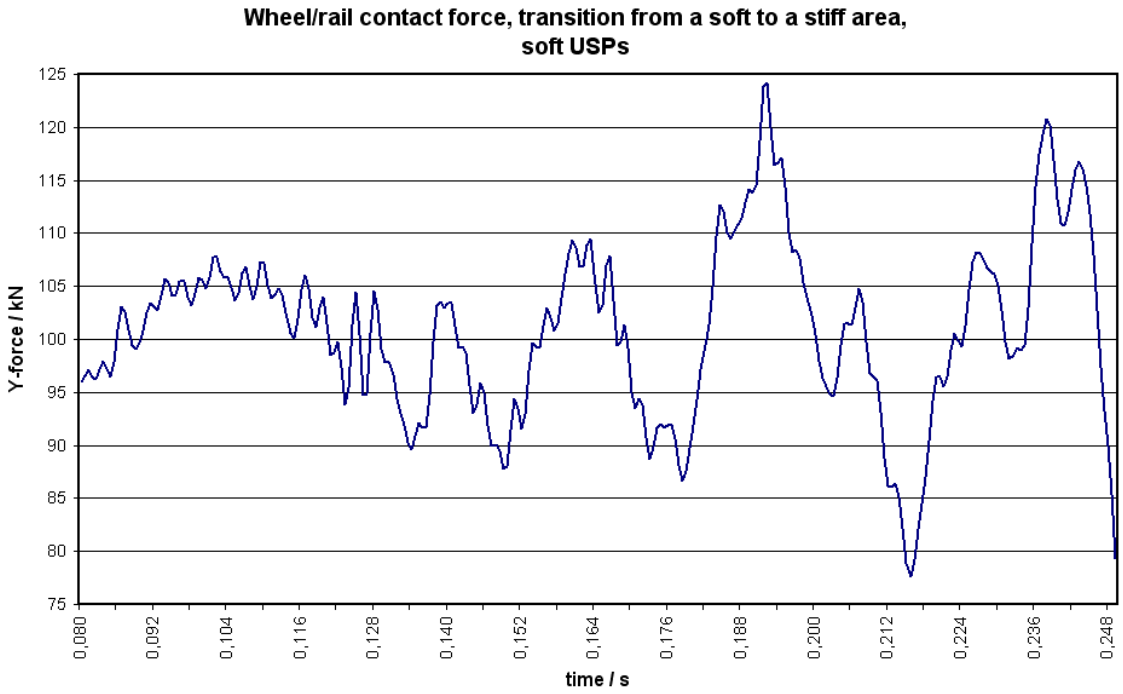

Figure 7.5: Vertical wheel/rail contact force with soft USPs at a transition

With soft USPs (Figure 7.5) the wheel/rail contact force oscillates on the soft part with a longer period than with medium USPs. There is no visible peak at the transition zone. But on the stiff part of the track the contact force variations increase.

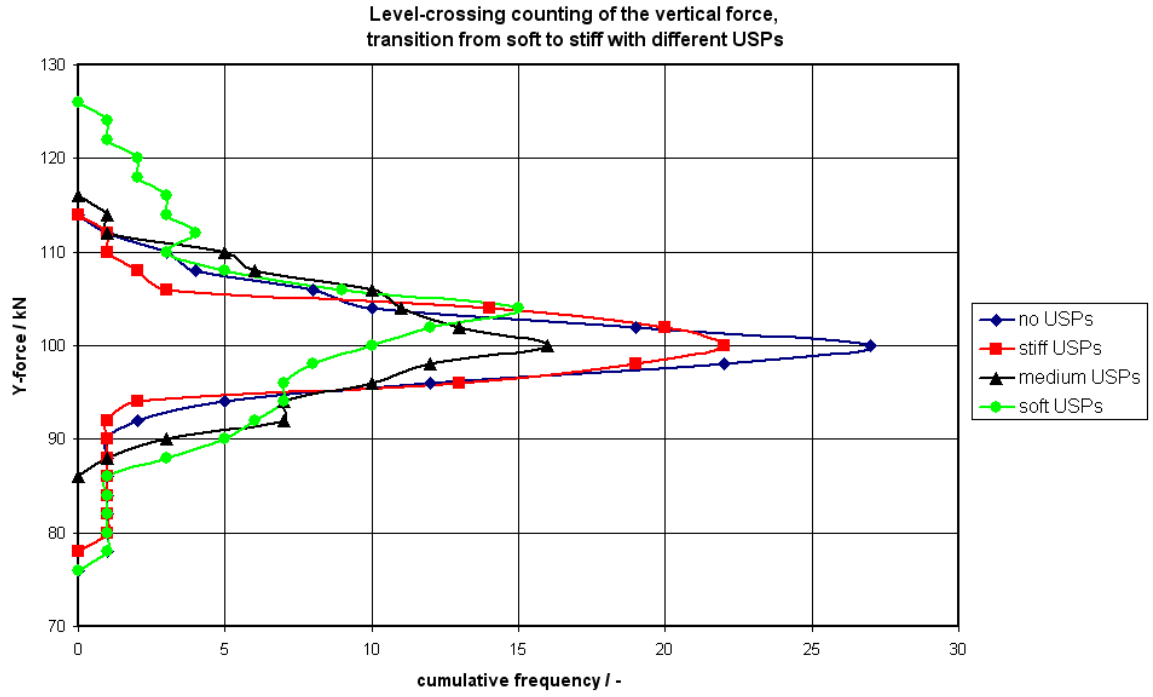

Figure 7.6: Level-crossing counting of the vertical wheel/rail contact force at a transition

In Figure 7.6 the result of the level-crossing counting for all four cases is shown. One can see that with softer USPs the number of oscillations with higher ranges increases. Without USPs or with stiff USPs the number of oscillations with small ranges is higher. The maximum range is 50 kN and is obtained when using soft USPs. With medium USPs the maximum range is the lowest of all examined cases. It is 30 kN in this case.

	no USPs	**stiff USPs**	**medium USPs**	**soft USPs**
mean	100.016 kN	100.000 kN	100.172 kN	100.994 kN
standard deviation	4.969	4.747	5.205	8.291

Table 7.2: Mean and standard deviation of contact force on a soft to stiff transition

Table 7.2 shows the mean value and the standard deviation of the examined contact forces. It is seen that the mean value and the standard deviation do not differ very much for the first three cases. But when using soft USPs both values increase. Especially the standard deviation increases highly when using soft USPs.

7.2.2 Ballast contact force

In this section the influence of the different USPs on the ballast contact force is investigated. Especially, the two ballast sections ten (at sleeper 10) and twenty (at sleeper 20) are examined. The section ten is located in the soft part of the track and the section twenty is located in the stiff part.

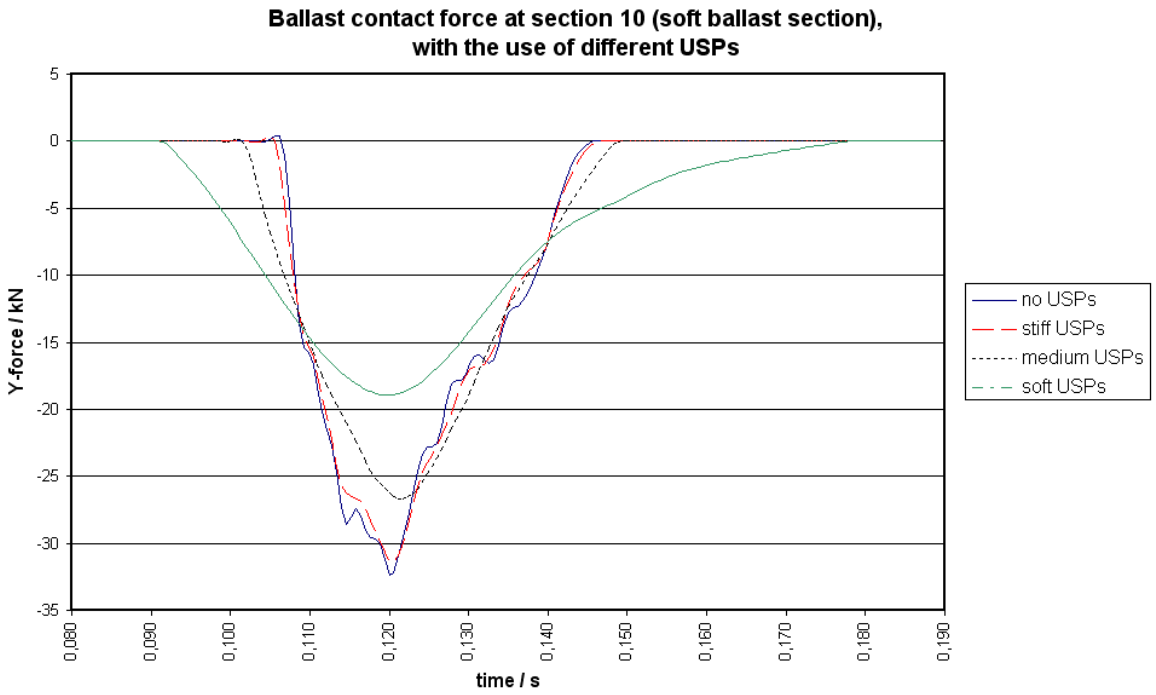

Figure 7.7: Ballast contact force at section ten

The Figure 7.7 shows the ballast contact force at section ten. One can see that the contact forces of using no USPs and stiff USPs are quite similar. They have both an extreme value, henceforth called maximum value, of -32 kN. With using softer USPs the maximum contact force decreases and the time of loading becomes longer. With medium USPs the maximum value of the contact force is -27 kN and with soft USPs -19 kN. The loading times increase from 0.041 s without USPs to 0.087 s with soft USPs.

The ballast contact force on the twentieth section is shown in Figure 7.8. One can see that the maximum forces increase compared to the soft section ten. The maximum force without using USPs is now -47 kN. There is now a clear difference between no USPs and stiff USPs. With stiff USPs the maximum contact force is -43 kN and with medium USPs it is -34 kN. With the soft USPs the maximum contact force is now -22 kN. The loading times increase again by using softer USPs. They go in this case from 0.027 s to 0.059 s.

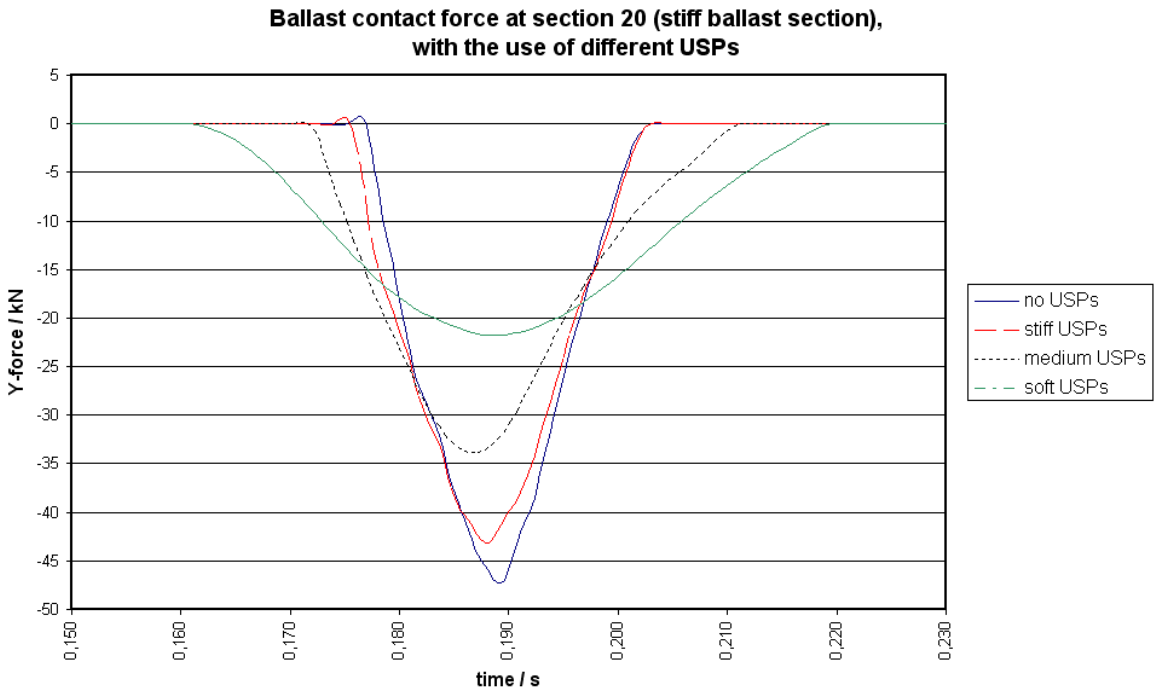

Figure 7.8: Ballast contact force at section twenty

7.3 Results

Summing up all these points it is obvious that the USPs influence the contact forces on a soft to stiff transition, for example an embankment to bridge transition, of a railway track. With softer USPs the peak in the contact force caused by the transition gets smaller, but on the other hand the wheel/rail contact force gets higher ranges and longer periods. The best results for the contact force is achieved with medium USPs. Hereby also the maximum range becomes the smallest of all examined cases, while softer USPs cause much higher oscillations with higher ranges. With stiff USPs compared to no USPs, there are almost no differences of the wheel/rail contact forces.

Also, it is obvious that with softer USPs the maximum ballast contact force decreases considerably and the time of loading increases. Therefore, with softer USPs the load from the train is distributed to more ballast sections. It is also seen that the ballast contact force increases when the ballast itself becomes stiffer. On a stiffer track there is almost no difference between using stiff USPs and no USPs.

8 Random track stiffness

8.1 Explanation

In this section the influence of randomly varying track stiffness is regarded. As shown in Chapter 4 the track stiffness varies along a railway track (see Figure 4.1 on page 8). Also, the track stiffness is influenced by switches, crossovers and track transitions. These variations of stiffness have an influence on the wheel/rail contact force. By increasing the wheel/rail contact force variations and causing higher vibrations in the railway track, a faster track degradation and track settlement will occur. An idea to reduce the variations of track stiffness is to use USPs. These are proposed to reduce the arising vibrations and distribute the forces of the train to more sleepers.

In the following part a railway track with random stiffness is investigated. Therefore Young's modulus of every section of the ballast in the track model used is changed. Each section will be given its own individual value of Young's modulus. An even distribution of Young's modulus is used with a minimum limit of 50 MPa and a maximum limit of 150 MPa. The values of Young's modulus for all the thirty sections of the model are calculated with the software *MATLAB*. The mean of the Young's modulus is set to be about 100 MPa. To investigate the influence of the USPs the wheel/rail contact force and the ballast contact forces are investigated. For analysing the wheel/rail contact force a level-crossing counting is done and the mean and standard deviation are calculated. As mentioned in Chapter 6 only the time between 0.08 s and 0.25 s is observed.

8.2 Calculations

8.2.1 Rail/wheel contact force

In Figure 8.1 the used Young's moduli of the thirty sections are shown. The changes of the Young's moduli differ between different sections. The smallest change is between

section 12 and 13 and it is only 2.6 MPa. The largest change is between section 20 and 21 and it is 95.0 MPa. The mean of the Young's moduli is 100.9 MPa and the average change between two nearby sections is 36.0 MPa.

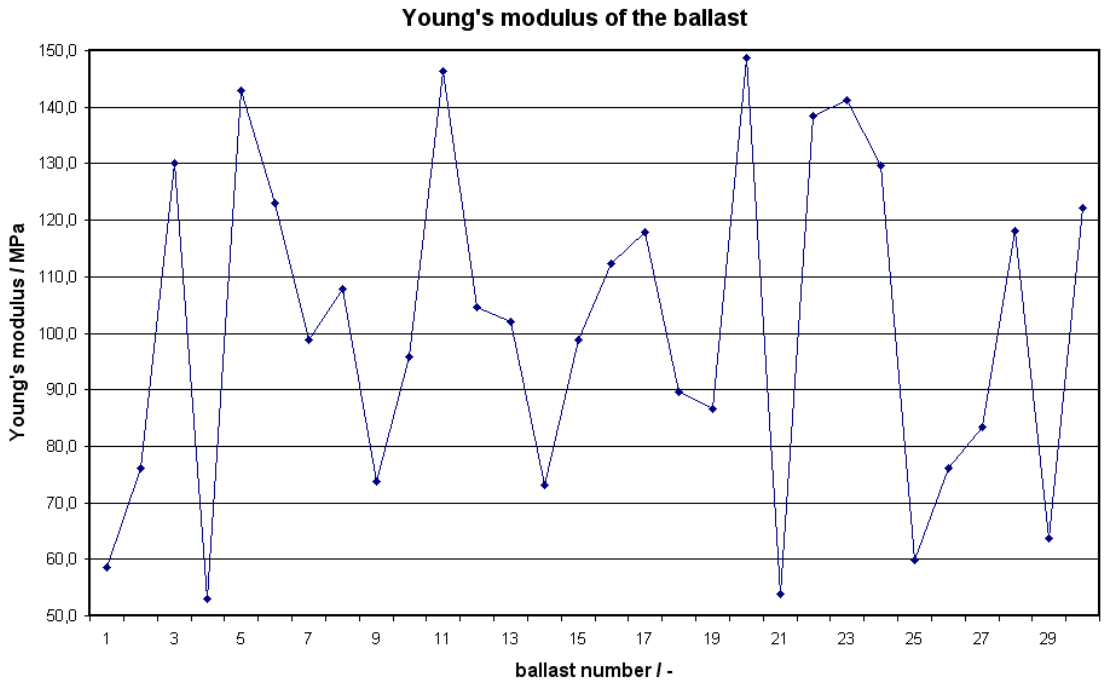

Figure 8.1: Variation of ballast's Young's modulus

Three calculations are done with different types of USPs and one calculation is done without using any USPs. The three different USPs are the same as used in Chapter 7: stiff, medium and soft ones. For the values of the USPs see Table 7.1 on page 16.

In Figure 8.6 the load spectrum of the level-crossing counting for all four time signals are shown. Without USPs the maximum verical force is 117 kN and the minimum one is 87 KN. Therefore the maximum range is 30 kN. The range of the oscillations become continuously smaller. The highest cumulative frequency is 20 oscillations at 100 kN and 101 kN. The load spectrum of the stiff USPs is almost the same as the one using no USPs. The maximum vertical force is 116 kN and the minimum one is 90 kN. So the maximum range is 26 kN. When using stiff USPs the maximum cumulative frequency increases to 22. The load spectrum for the medium USPs has a lower maximum range of only 20 kN. The range lays between 110 kN and 90 kN. In the area from three oscillations and more the load spectrum is almost the same as the two load spectra of no USPs and stiff USPs. But some more small oscillations are counted. When using soft USPs the ranges increase. There are more oscillations with high ranges counted.

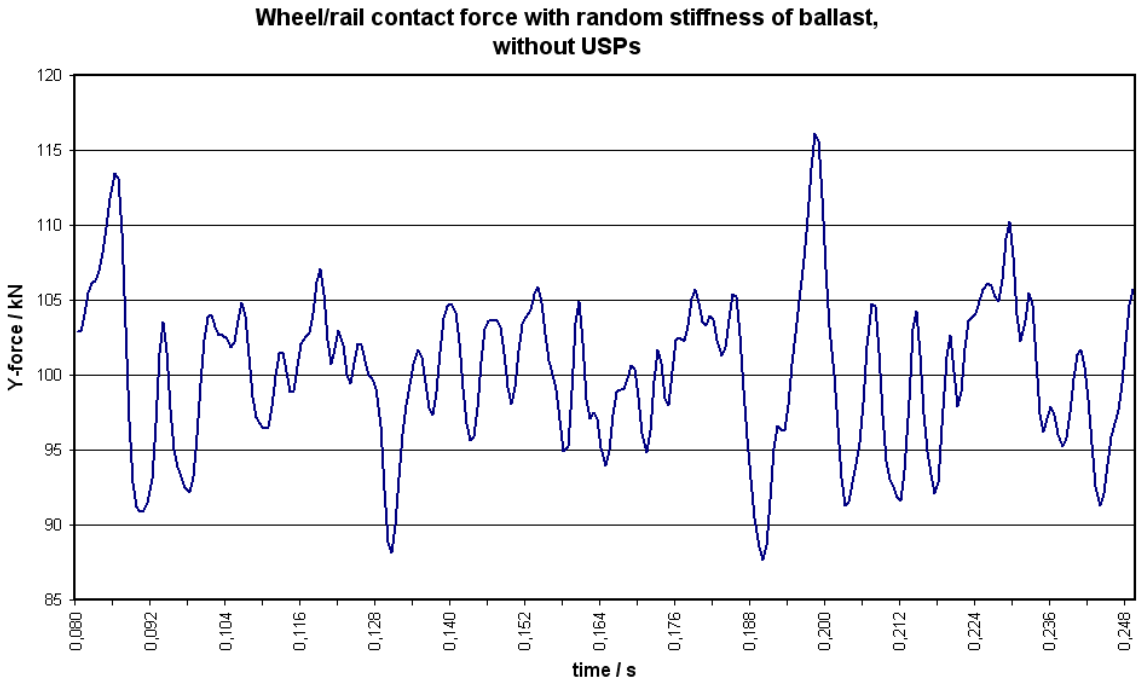

Figure 8.2: Vertical wheel/rail contact force with variation of ballast's stiffness and no USPs

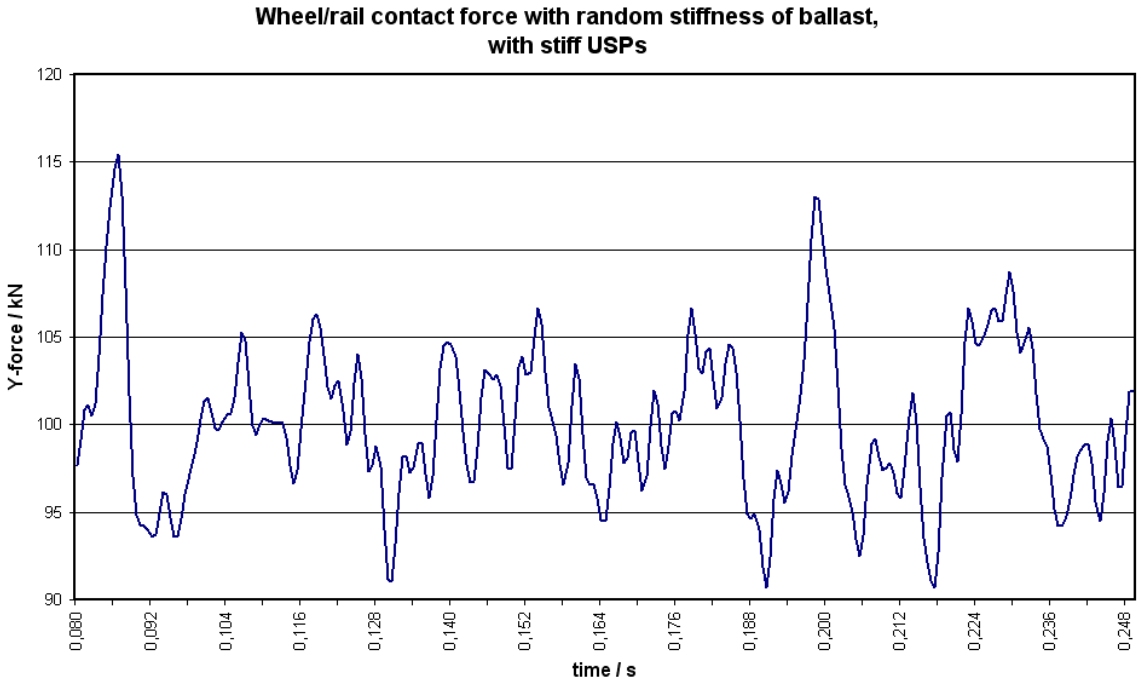

Figure 8.3: Vertical wheel/rail contact force with variation of ballast's stiffness and stiff USPs

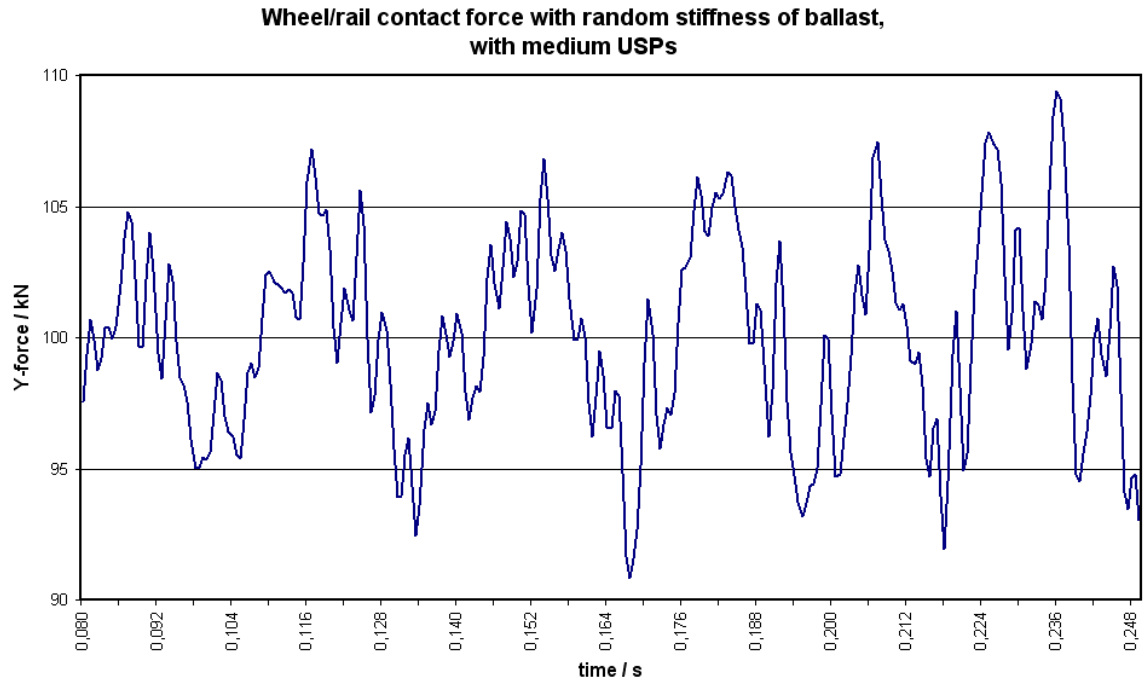

Figure 8.4: Vertical wheel/rail contact force with variation of ballast's stiffness and medium USPs

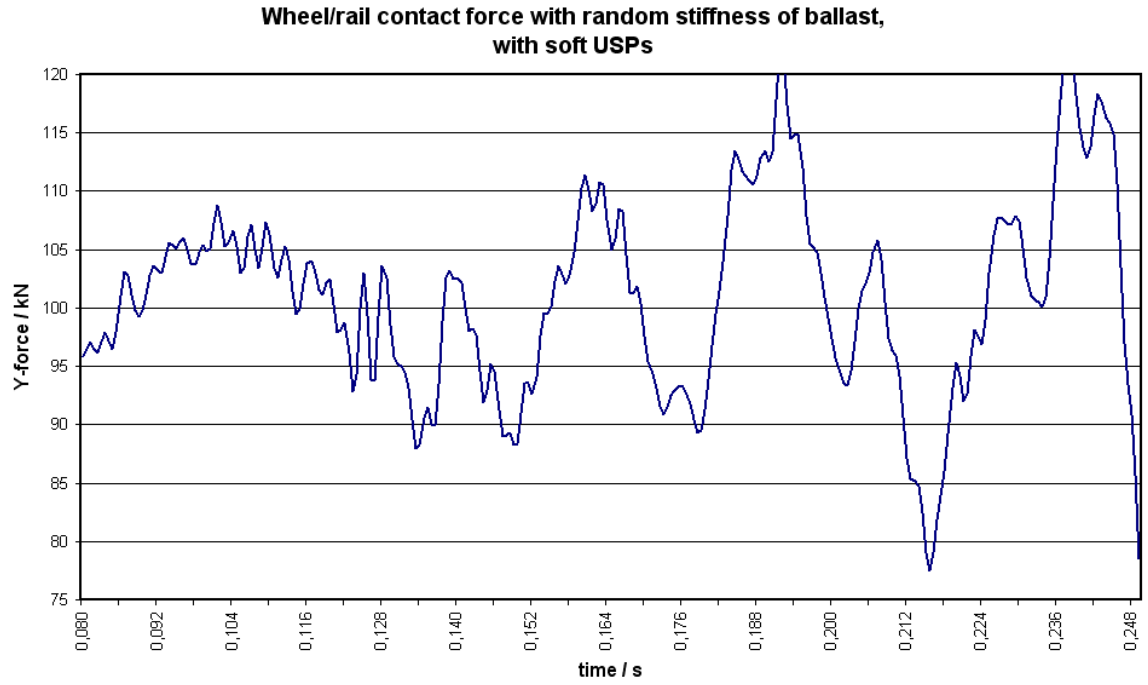

Figure 8.5: Vertical wheel/rail contact force with variation of ballast's stiffness and soft USPs

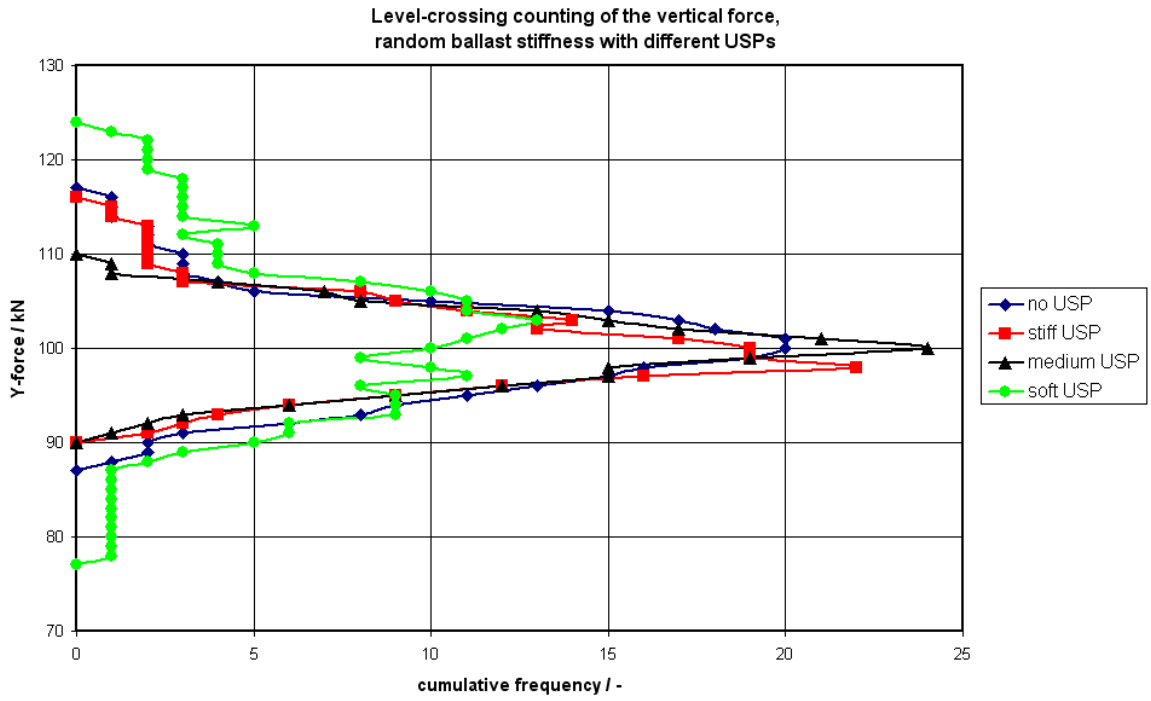

Figure 8.6: Level-crossing counting of the vertical wheel/rail contact force

But the number of small oscillations decreases. The maximum vertical force becomes 124 kN and the minimum one 77 kN. Therefore the maximum range is 47 kN.

	no USPs	**stiff USPs**	**medium USPs**	**soft USPs**
mean	100.115 kN	100.071 kN	100.037 kN	101.014 kN
standard deviation	5.081	4.477	3.767	8.470

Table 8.1: Mean and standard deviation of contact force on a random track

In Table 8.1 the mean values and the standard deviations are shown for all four cases. One can see that the differences between the mean values in the first three cases are very small. With using soft USPs there is a small increase of the mean value of the contact force. The standard deviation when using stiff USPs becomes lower than when no USPs are used. With medium USPs the standard deviation is the lowest of all cases examined. When using soft USPs the standard deviation increases.

8.2.2 Ballast contact force

To analyse the ballast contact force two sleepers are examined. The sleeper 11 is located at a section with a high Young's modulus of 146.3 MPa whereas the sleeper 21

is located on a very soft section. The Young's modulus of this section is only 53.8 MPa. The calculated vertical forces are shown in Figure 8.7.

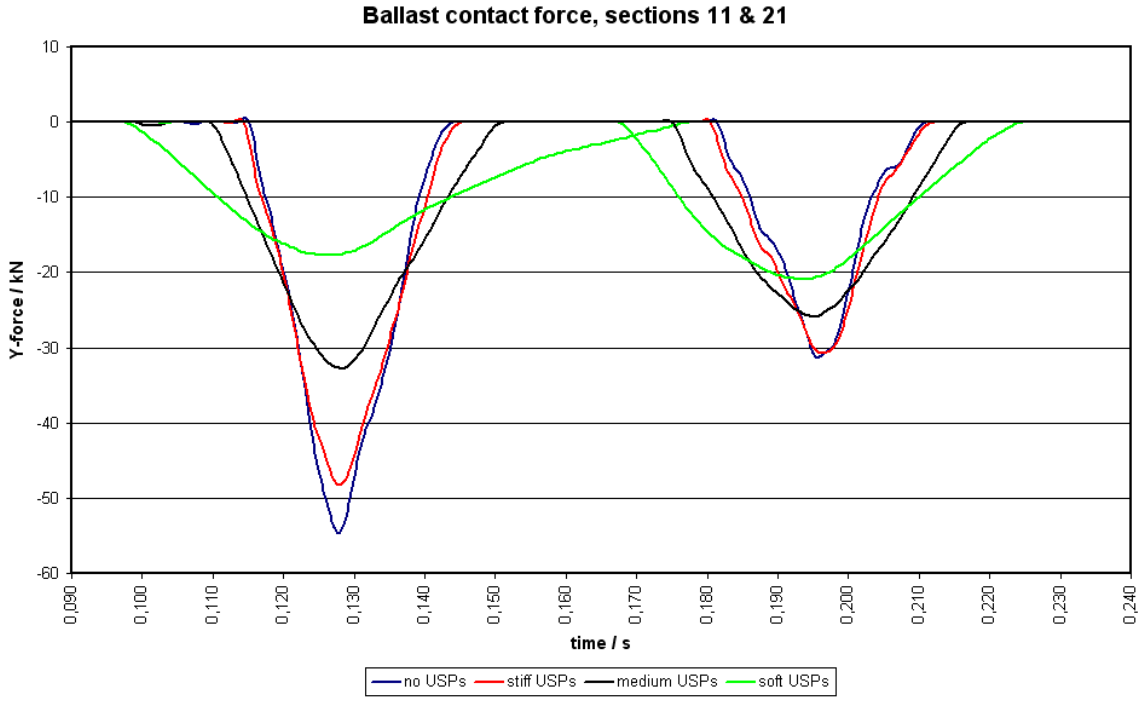

Figure 8.7: Ballast contact force at section eleven and twenty-one

The maximum force without using USPs is -55 kN at section 11 and -31 kN at section 21. By using stiff USPs the contact force is reduced to -48 kN on the stiff section, but on the soft section there is almost no change of the contact force and the maximum values keep constant. With medium USPs the maximum contact forces are reduced to -33 kN and -26 kN, respectively. Also the times of loading on both sections increase. When using soft USPs the maximum contact forces get further reduced to -18 kN on section 11 and to -21 kN on section 21. Also the time of loading increases further.

8.3 Results

To sum up the four simulations one can see that the difference on the wheel/rail contact force between using no USPs and stiff ones is small. When using medium USPs the mean value keeps almost constant compared to using no USPs. But the standard deviation decreases. Also, the maximum range is the lowest and the force variations are the smallest of all four cases. Soft USPs have a great influence on the wheel/rail contact force. The maximum range of the force increase but fewer oscillations are

counted and the standard deviation increases considerably. Regarding all these points one can see that the wheel/rail contact force variations increase when using soft USPs. With medium USPs the contact force gets the best values. In this case the maximum range of the oscillation is minimum.

When using USPs the maximum ballast contact force decreases and the time of loading increases. The influence of the ballast stiffness is also visible: with increasing stiffness of the ballast the ballast contact force also is increased. When using soft USPs the maximum forces at both sections differ by 3 kN only, whereas the difference is 24 kN without using USPs. For all four cases, the differences of the ballast contact forces are smaller on the soft section than on the stiff section.

9 Hanging sleepers

9.1 Explanation

In this chapter the influence of hanging sleepers on the contact forces is investigated. A hanging sleeper is unsupported and has no direct contact to the ballast. There is a gap between the sleeper and the ballast. Hanging sleepers are a result of track settlement. Under the load of the passing trains the track settlement is not the same in every section because of variations of the ballast stiffness. Therefore some sleepers may not be fully supported and some may even lose contact to the ballast bed. When a gap between the sleeper and the ballast exists, this can be closed by the load of a passing train. The ballast then carries some of the load as soon as the gap is closed. But if the gap is not closed no forces will be carried by the ballast in this section. At hanging sleepers the vertical track stiffness becomes very low. These changes of the vertical track stiffness cause high train/track interaction forces, which will increase the track settlement rate (see also Chapter 3). One task of the sleepers is to distribute the forces of the train into the ballast. If one sleeper is hanging, the sleepers next to the hanging one will carry higher forces. Therefore the ballast under these sleepers is highly stressed. This can also lead to a faster ongoing track settlement.

In this work three different cases of hanging sleepers are investigated. In the first case only one sleeper is hanging. In the second case three hanging sleepers are placed in a line. Finally the case of one supported sleeper, placed between two hanging sleepers, is investigated. For all three cases the wheel/rail contact forces for using no, stiff and medium USPs are examined. Furthermore the ballast contact forces for using no, stiff, medium and soft USPs are examined. The USPs have the same properties as mentioned in Chapter 7.

In this work hanging sleepers are simulated by reducing the ballasts' Young's moduli of the sections. For ballast sections which should have a hanging sleeper the Young's modulus is set to 0.1 MPa instead of 100 MPa in the sections with supported sleepers. Because of the low Young's modulus the ballast does not carry forces from the sleeper.

This simulates a total hanging sleeper with a gap that does not get closed under the load of the passing trains.

9.2 Calculations of the wheel/rail contact force

9.2.1 One hanging sleeper

The sleeper number 12 is hanging in this example. The hanging sleeper is reached by the wheel after 0.135 s. The calculated wheel/rail contact forces for all three investigated cases are shown in Figure 9.1.

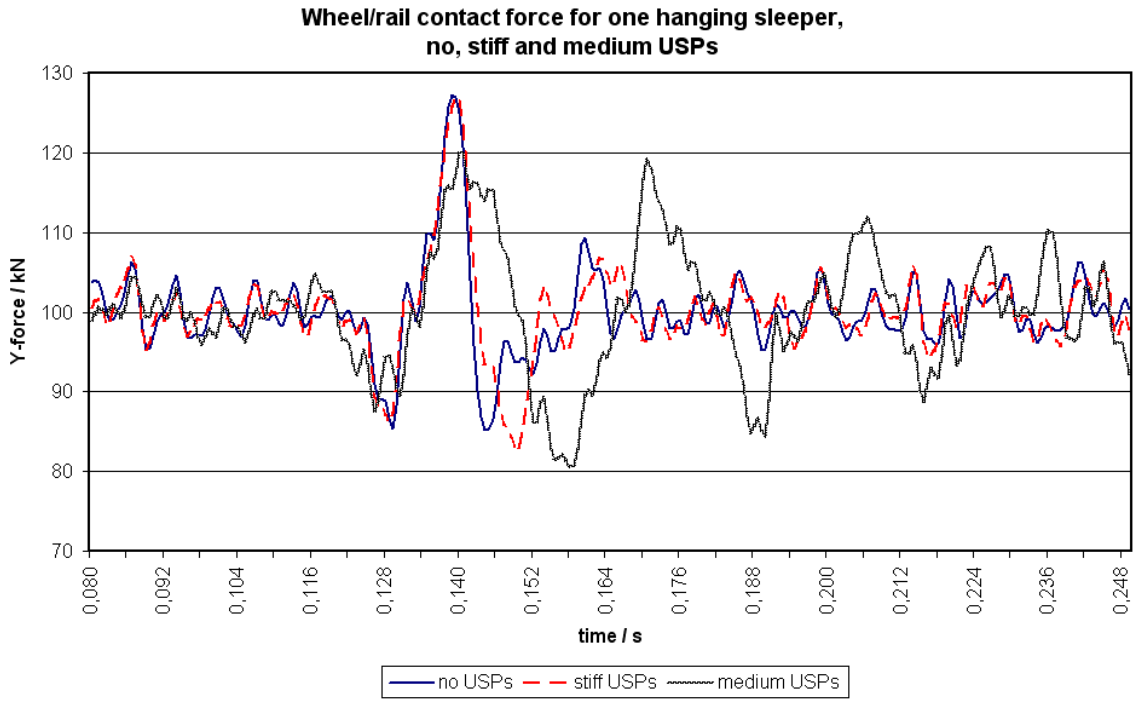

Figure 9.1: Vertical wheel/rail contact force for one hanging sleeper

When not using USPs the wheel/rail contact force goes down to 85 kN after 0.130 s. At this time the wheel is at sleeper 11. Afterwards the contact force rises up to 127 kN at time 0.140 s. At his time the wheel is located between the sleeper 12 and 13. Afterwards the contact force decreases again to 85 kN at 0.145 s. The maximum range caused by the hanging sleeper is therefore 42 kN.

The contact force when using stiff USPs is similar to the one obtained when using no USPs. Before reaching the hanging sleeper the contact force falls to 86 kN. The maximum force becomes 127 kN as for using no USPs. Afterwards the contact force

falls to 83 kN and becomes even lower than for using no USPs. Therefore the maximum range increases to 44 kN. Also, there is a small time shift between the two curves. The minimum contact force now appears at 0.150 s.

With the use of medium USPs the peak of the contact force caused by the hanging sleeper is lower. In front of sleeper 12 the force decreases to 88 kN and becomes 120 kN after the hanging sleeper. Thereafter the contact force decreases to 81 kN. The maximum range is therefore 39 kN. After the wheel has passed the hanging sleeper the contact force oscillates with a higher amplitude and a longer time period.

9.2.2 Three adjacent hanging sleeper

In this example the sleepers 11, 12 and 13 are hanging. The first hanging sleeper is reached by the wheel after 0.130 s. The wheel/rail contact forces are shown in Figure 9.2.

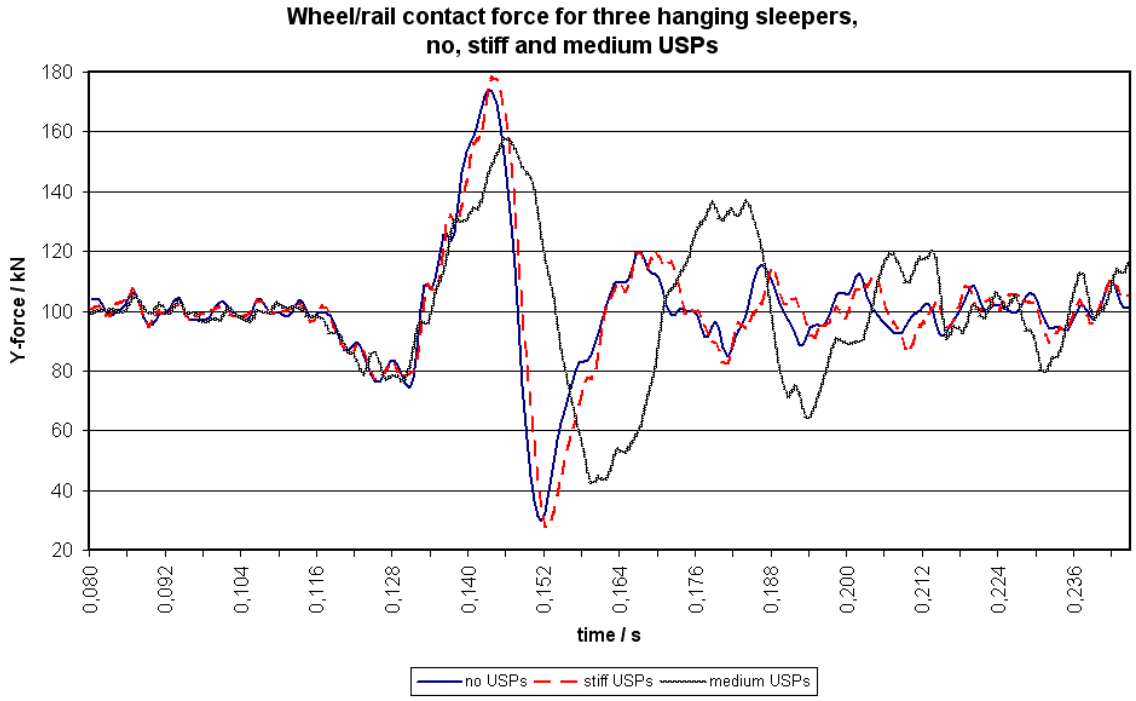

Figure 9.2: Vertical wheel/rail contact force for three hanging sleepers

The wheel/rail contact force when using no USPs decreases in front of the hanging sleepers. In front of the hanging sleepers the contact force now goes down to 74 kN. Afterwards the contact force increases constantly to 174 kN at 0.143 s. At this time the wheel has just left the last hanging sleeper. Then the force decreases rapidly to

30 kN at 0.152 s when the wheel is located at sleeper 14. Then the oscillation of the contact force decreases. The maximum range caused by the three hanging sleepers is 144 kN.

When using stiff USPs there are only small changes of the contact force as compared to using no USPs. The minimum contact force in front of the hanging sleepers is now 77 kN. The maximum contact force becomes 178 kN and falls down to 28 kN afterwards. Therefore the maximum range caused by the hanging sleepers rises to 150 kN. After the wheel has passed the hanging sleepers the contact force decreases to what one obtains when not using any USPs.

The contact force when using medium USPs looks similar to the two other curves in front of the hanging sleepers. The contact force goes down to 77 kN. But the maximum force is now lower than in the two other cases. It increases to 157 kN only at 0.146 s. Afterwards the contact force goes down to 42 kN at 0.160 s. Therefore the maximum range becomes 115 kN. After the section with the hanging sleepers the contact force oscillates with higher amplitudes and longer time periods than it does when using no or stiff USPs.

9.2.3 Two hanging sleepers with one supported between them

In this case one supported sleeper is surrounded by one hanging sleeper on each side. The supported sleeper is number 12 while the sleepers 11 and 13 are hanging. The forces of all three calculations are shown in Figure 9.3.

Like in the first two cases of hanging sleepers considered the contact forces decrease in front of the first hanging sleeper in all calculations. They becomes 87 kN without USPs, 85 kN with stiff USPs and 89 kN with medium USPs. After the first hanging sleeper the contact forces rise up to 118 kN when using no USPs and up to 117 kN when using stiff USPs. At the supported sleeper 13 the wheel/rail contact force falls down to 83 kN without the use of USPs. With using medium USPs the contact force goes down to 97 kN only. Afterwards both contact forces rise again. The second maximum is 124 kN when using no USPs and 118 kN when using stiff USPs, respectively afterwards the amplitudes of both forces become lower, whereby the contact force when using stiff USPs goes down faster. When using soft USP the contact force rises slower when the hanging sleepers are passed. There is only one peak when the wheel leaves the supported sleeper in the middle after 0.140 s. The maximum force becomes 117 kN. Afterwards the force decreases to 76 kN at time 0.162 s. The contact force when using

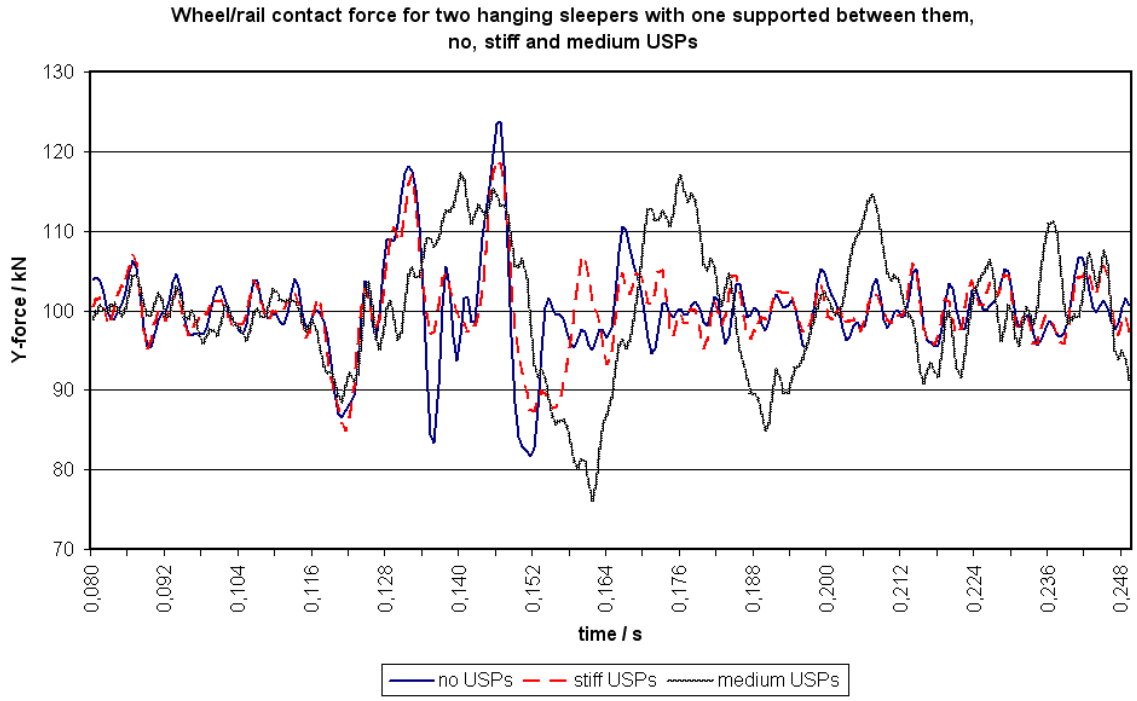

Figure 9.3: Vertical wheel/rail contact force with two hanging sleepers and one supported between them

medium USPs oscillates with higher amplitudes and has a longer period time after the wheel has passed the hanging sleepers.

9.3 Calculations of the ballast contact force

9.3.1 One hanging sleeper

In the following the contact forces between the sleepers and the ballast will be investigated for the case of one hanging sleeper at section 12. Therefore the contact forces at the sleepers 10, 11, 13, 14 and 15 are examined. The contact forces of these sleepers are shown in the Figures 9.4 to 9.7 for all types of USPs and no USPs used.

In Figure 9.4 it is seen that the maximum contact force without using USPs increases from -46 kN at sleeper 10 to -52 kN at sleeper 11 in front of the hanging sleeper. The highest maximum contact force is measured at sleeper 13 with -78 kN. This sleeper is the first one after the hanging sleeper. Afterwards the maximum force decreases to -47 kN at sleeper 14 and to -45 kN at sleeper 15. Thus the contact force is back to the level it was at sleeper 10.

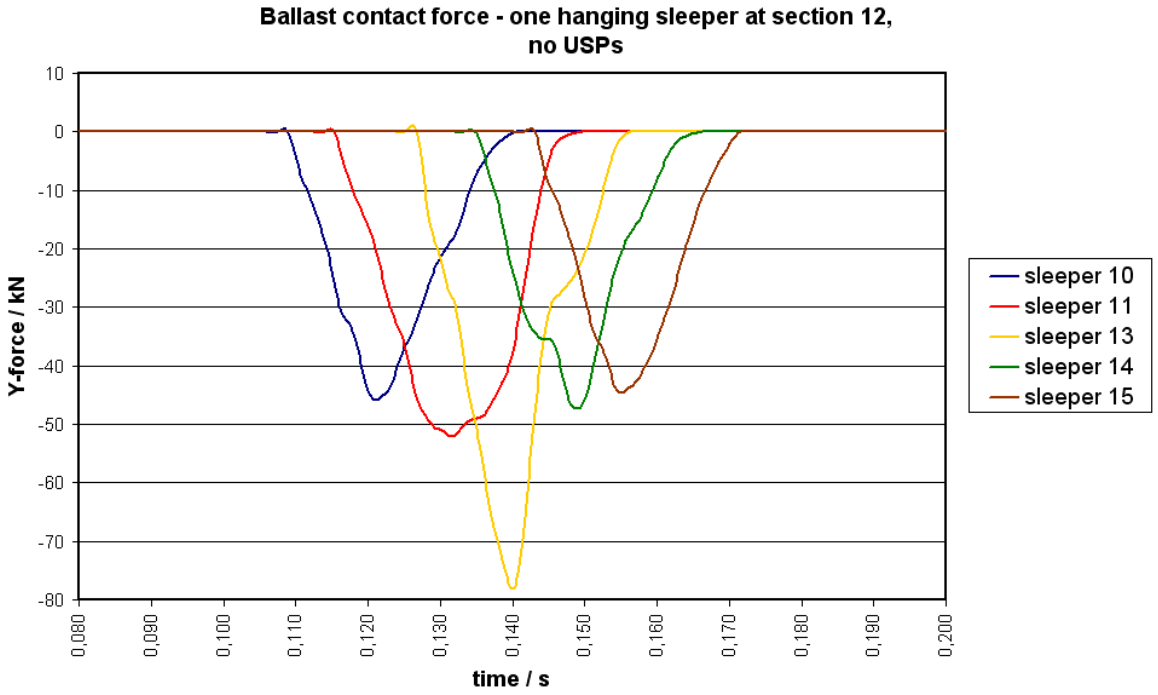

Figure 9.4: Ballast contact force for one hanging sleeper and no USPs

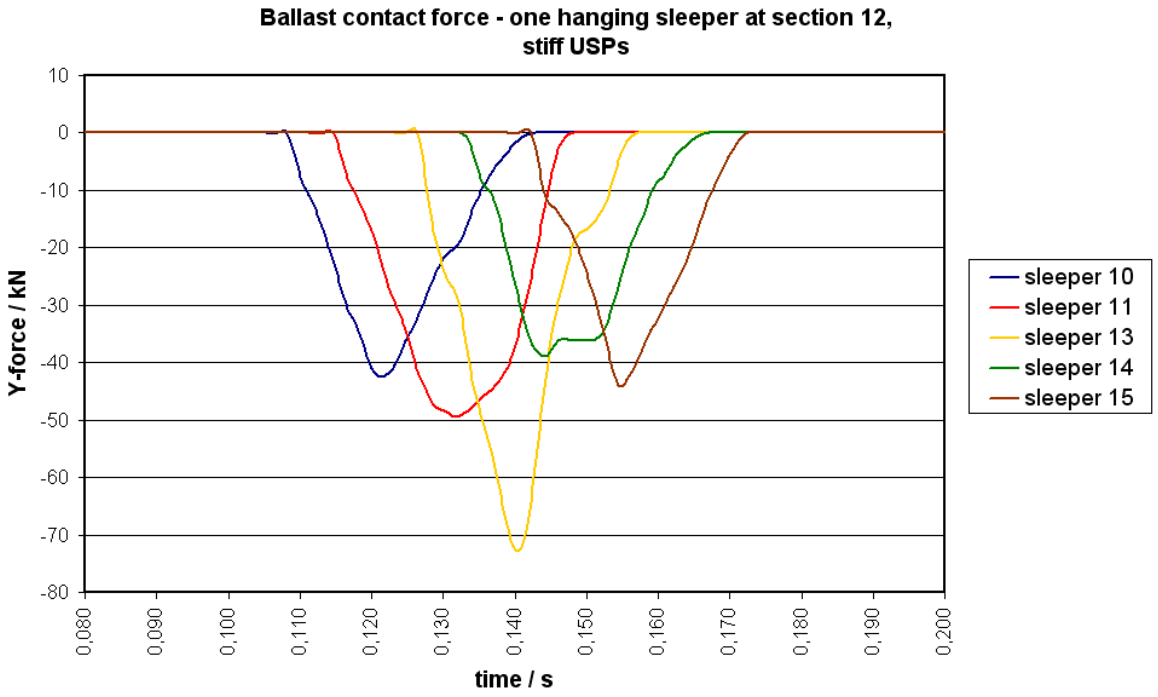

Figure 9.5: Ballast contact force with one hanging sleeper and stiff USPs

In Figure 9.5 the contact forces for using stiff USPs are shown. The behaviour of the contact forces is similar to the case with no USPs, but the forces are a little bit lower. At sleeper 10 the maximum force is now -42 kN and it rises to -49 kN at sleeper 11. The highest force is again obtained at sleeper 13 with -73 kN. The contact force on sleeper 14 decreases to -39 kN and at sleeper 15 to -44 kN. Noticeable is that the maximum contact force at sleeper 14 is the smallest one of all forces shown.

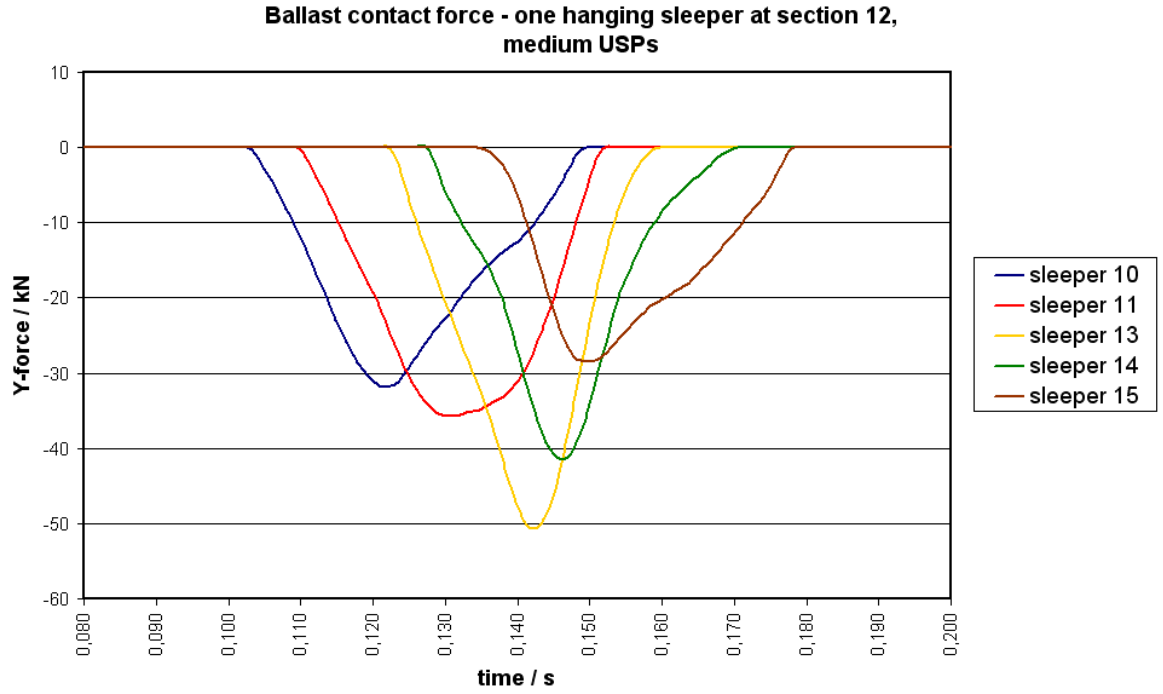

Figure 9.6: Ballast contact force with one hanging sleeper and medium USPs

The contact forces when using medium USPs are shown in Figure 9.6. The maximum contact forces in front of the hanging sleepers are -32 kN at sleeper 10 and -36 kN at sleeper 11. The maximum contact force when using medium USPs is -51 kN at sleeper 13. In this case the contact force decreases slower after sleeper 13. At sleeper 14 the maximum contact force is still -41 kN. But at sleeper 15 the maximum contact force decreases to -28 kN and is even lower than in front of the hanging sleeper.

The contact forces when using soft USPs are shown in Figure 9.7. The maximum contact forces at sleeper 10 and 11 are both -19 kN. At sleeper 13 the maximum contact force increases lightly to -21 kN. Afterwards the maximum contact forces do not decrease as in the other cases. At sleeper 14 the maximum contact force keeps constant at -21 kN and at sleeper 15 it is -22 kN.

In Table 9.1 all maximum contact forces of the ballast are shown for the case of one hanging sleeper.

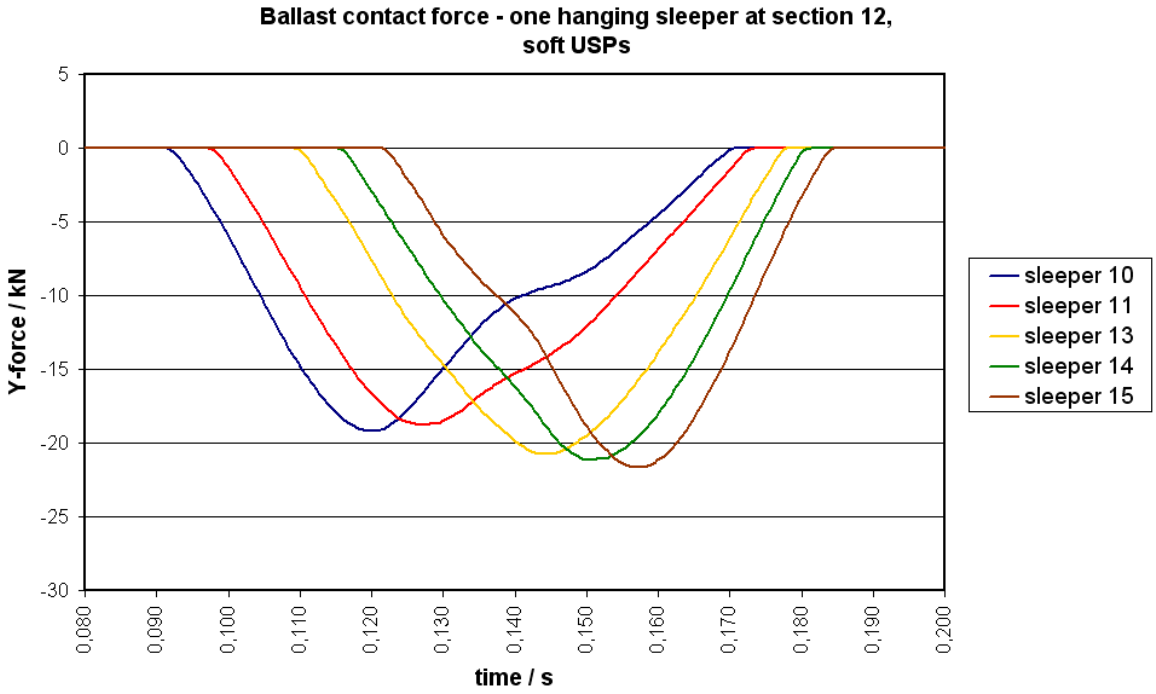

Figure 9.7: Ballast contact force with one hanging sleeper and soft USPs

USPs	no	stiff	medium	soft
sleeper 10	-46 kN	-42 kN	-32 kN	-19 kN
sleeper 11	-52 kN	-49 kN	-36 kN	-19 kN
sleeper 13	-78 kN	-73 kN	-51 kN	-21 kN
sleeper 14	-47 kN	-39 kN	-41 kN	-21 kN
sleeper 15	-45 kN	-44 kN	-28 kN	-22 kN

Table 9.1: Maximum ballast contact forces with one hanging sleeper

9.3.2 Three adjacent hanging sleepers

The two sleepers 9 and 10 before the three hanging sleepers and the three sleepers 14, 15 and 16 after the three hanging sleepers are examined. The contact forces for all four cases are shown in the Figures 9.8 to 9.11.

The ballast contact forces when using no USPs are shown in Figure 9.8. In front of the three hanging sleepers the maximum contact force increase from -46 kN at sleeper 9 to -64 kN at sleeper 10. The loading time of sleeper 10 is very long compared to the other sleepers. The contact force becomes zero at almost the same time as the contact force of sleeper 14. The maximum contact force at sleeper 10 occurs when the wheel passes the three hanging sleepers. In comparison the loading of the contact force of

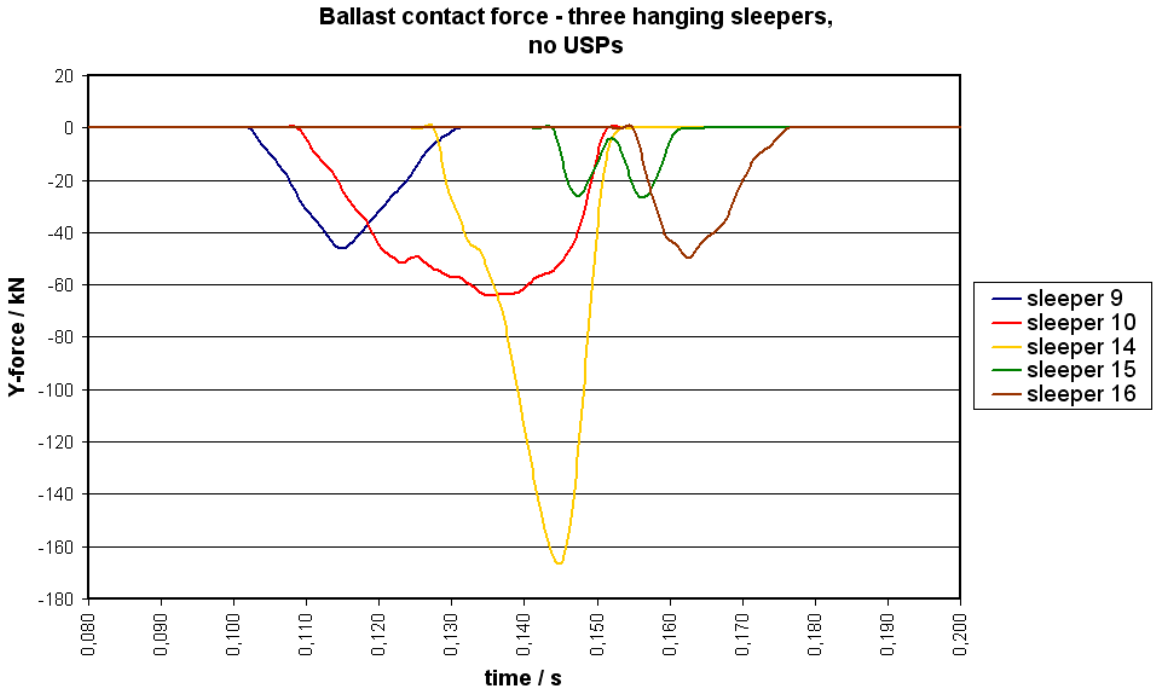

Figure 9.8: Ballast contact force with three hanging sleepers and no USPs

sleeper 14 is shorter. But the maximum contact force is much larger. It is -166 kN at this sleeper. At sleeper 15 the contact force becomes very low. It has a first peak of -26 kN at 0.148 s. Afterwards the force becomes almost zero before a second peak of also -26 kN occurs at time 0.156 s. Afterwards the contact force becomes normal at sleeper 15 again. The maximum contact forces is -50 kN at this sleeper.

The ballast contact forces when using stiff USPs are shown in Figure 9.9. The forces look similar to those obtained when using no USPs, but they are slightly lower. In front of the three hanging sleepers the maximum contact force increase now from -42 kN at sleeper 9 to -64 kN at sleeper 10. The loading time of sleeper 10 is again very long compared to the other sleepers. The contact force becomes zero at the same time as the force of sleeper 14. The maximum contact force at sleeper 10 occurs when the wheel has left the last hanging sleeper. In comparison, the loading of the contact force of sleeper 14 is again shorter. But again the maximum contact force is much larger and becomes -156 kN at this sleeper. Thus, the maximum contact force is now 10 kN lower than without using USPs. Afterwards the maximum contact forces decrease to normal values of -37 kN at sleeper 15 and -42 kN at sleeper 16.

In Figure 9.10 the ballast contact forces when using medium USPs are shown. The times of loading of the sleepers in front of the hanging section becomes longer. All examined contact forces becomes zero at almost the same time of 0.16 s. The maximum

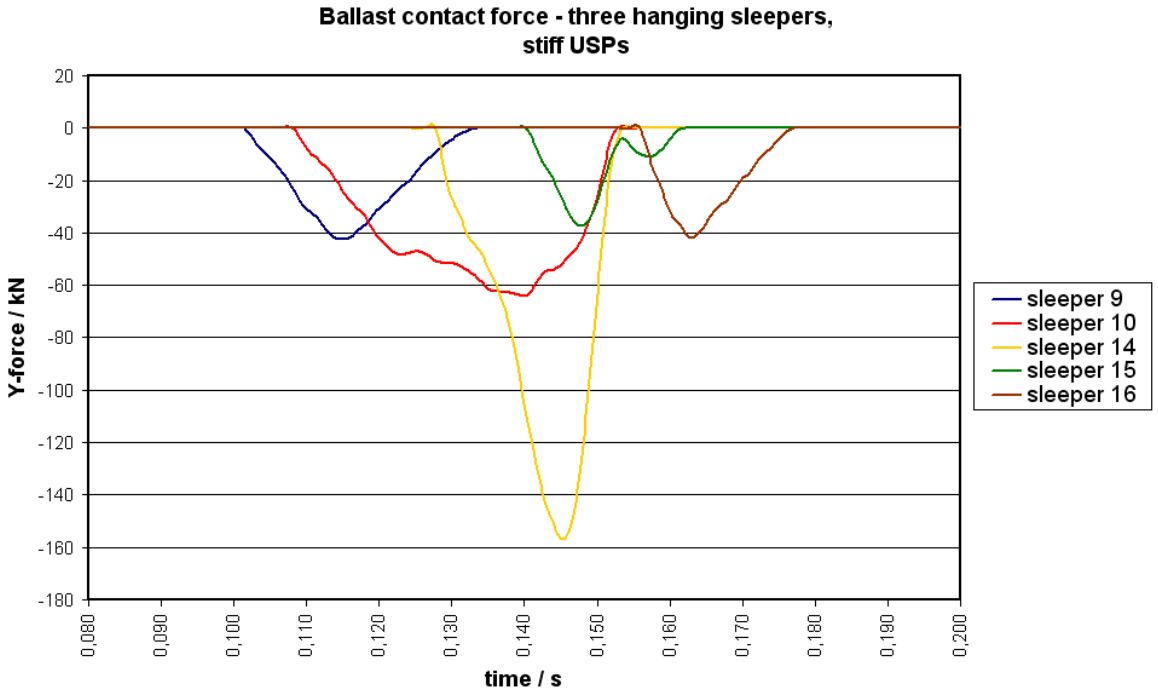

Figure 9.9: Ballast contact force with three hanging sleepers and stiff USPs

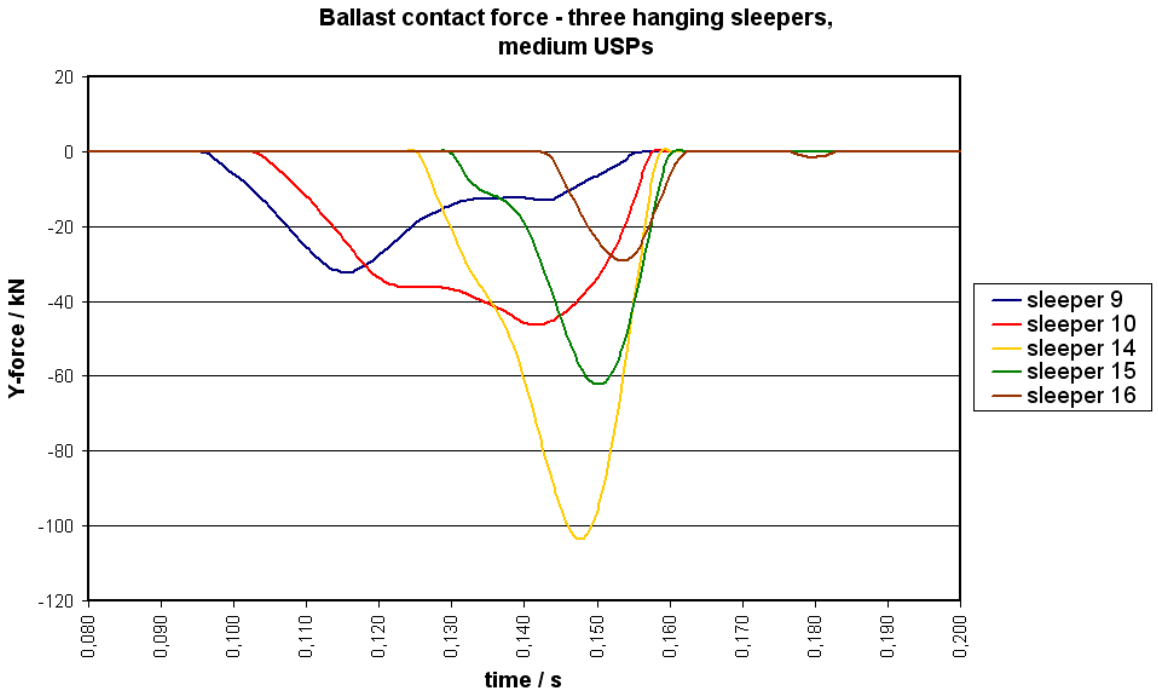

Figure 9.10: Ballast contact force with three hanging sleepers and medium USPs

contact force at sleeper 9 is -32 kN. The loading force at sleeper 10 increases while the wheel passes the hanging section and reaches its maximum value of -46 kN shortly before the wheel leaves the hanging section. When using medium USPs the maximum contact force at sleeper 14 decreases to -103 kN. In this case the maximum contact force at sleeper 15 increases. It is now -62 kN and this is even higher than when using no or stiff USPs. The maximum contact force at sleeper 14 is -29 kN. So it is lower than at sleeper 9 and has a much shorter loading time.

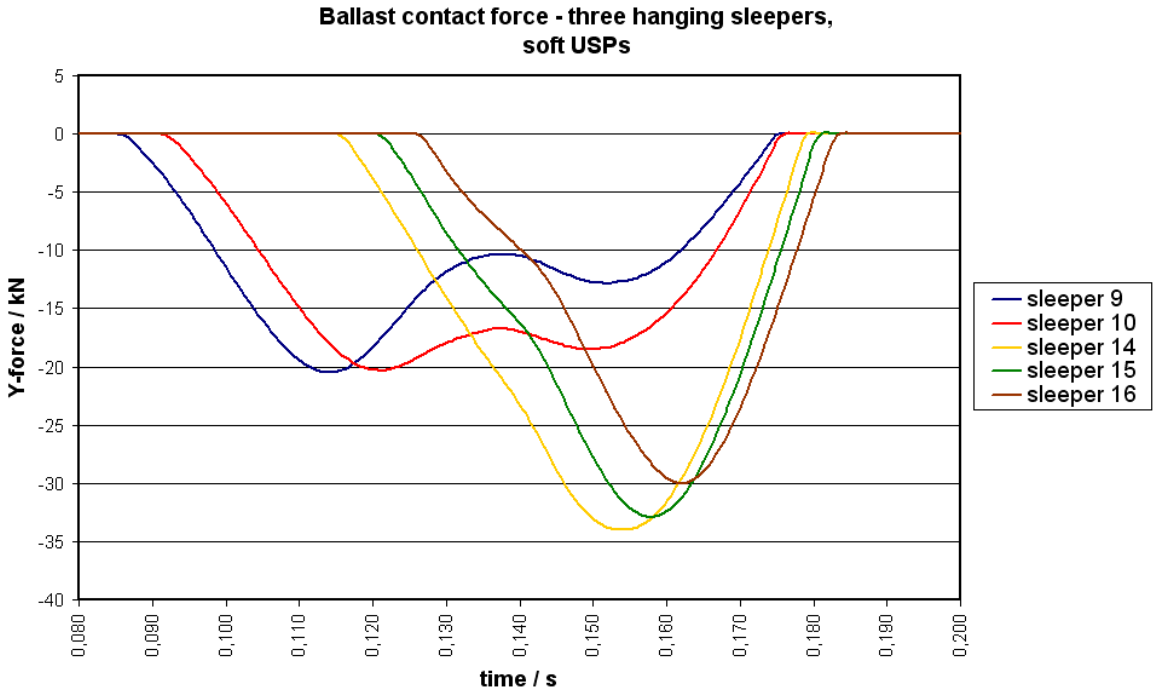

Figure 9.11: Ballast contact force with three hanging sleepers and soft USPs

When using soft USPs (Figure 9.11) the maximum ballast contact forces at sleeper 9 and 10 are -20 kN. Both contact forces have very long loading times and both become zero shortly before the contact force of sleeper 14 becomes zero. While the wheel passes the hanging section the contact force at sleeper 10 is about 5 kN higher than the one at sleeper 9. Both forces oscillate lightly. The maximum contact forces at the sleepers behind the hanging section are higher. The contact force has a maximum value of -34 kN at sleeper 14. On the following sleepers the maximum value of the contact forces decreases to -33 kN at sleeper 15 and to -30 kN at sleeper 16. The contact forces behind the hanging section are thereby more like a parable and have a shorter loading time.

For the case of three adjacent hanging sleepers the maximum ballast contact forces are shown in Table 9.2.

USPs	no	stiff	medium	soft
sleeper 9	-46 kN	-42 kN	-32 kN	-20 kN
sleeper 10	-64 kN	-64 kN	-46 kN	-20 kN
sleeper 14	-166 kN	-156 kN	-103 kN	-34 kN
sleeper 15	-26 kN	-37 kN	-62 kN	-33 kN
sleeper 16	-50 kN	-42 kN	-29 kN	-30 kN

Table 9.2: Maximum ballast contact forces with three hanging sleeper

9.3.3 Two hanging sleepers with one supported between them

In this section five sleepers are examined. The first two sleepers are number 9 and 10, which are located in front of the first hanging sleeper 11. The next one is the supported sleeper 12 between the two hanging sleepers. Besides the two sleepers 14 and 15 are examined. These two sleepers are located after the last hanging sleeper. The results are shown in the Figures 9.12 to 9.15.

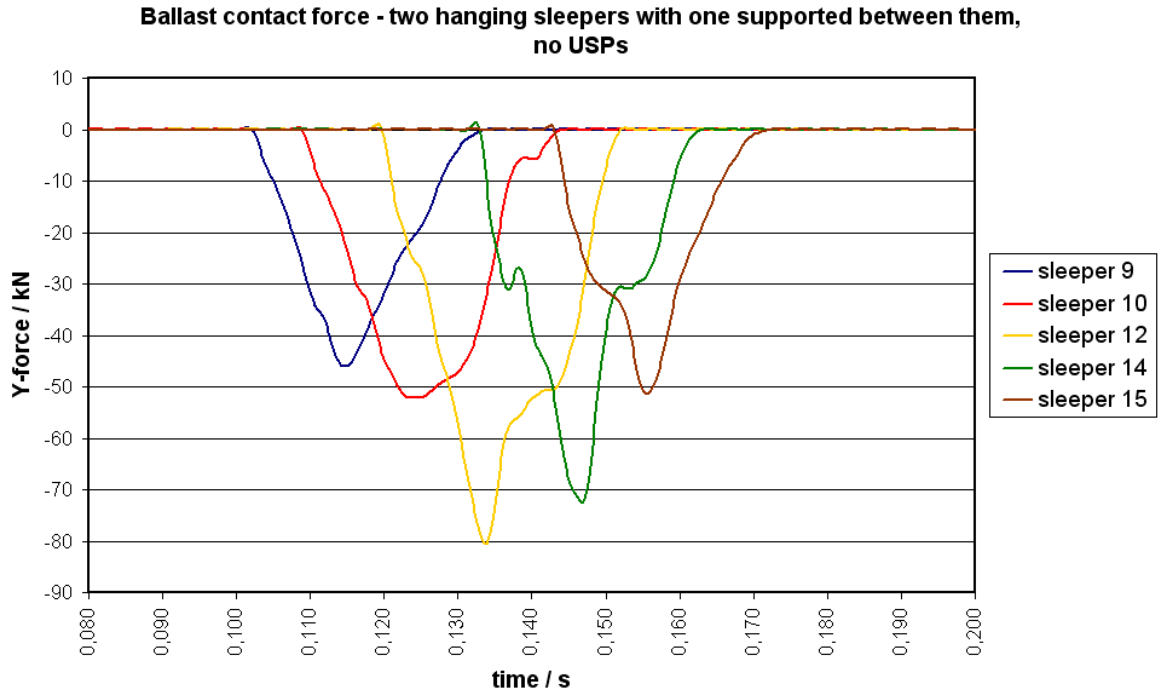

Figure 9.12: Ballast contact force with two hanging sleepers and no USPs

In Figure 9.12 the ballast contact forces are shown when using no USPs. In front of the first hanging sleeper the maximum contact force increases from -46 kN at sleeper 9 to -52 kN at sleeper 10. The contact force at sleeper 12 has a maximum of -80 kN. At sleeper 14 the maximum contact force decreases to -72 kN. At the sleeper 15 the

maximum contact force decreases to -51 kN and has therefore a value similar to the sleepers in front of the hanging sleeper section. The contact forces at the sleepers 12, 14 and 15 are more peaky than the contact forces in front of the hanging sleeper section.

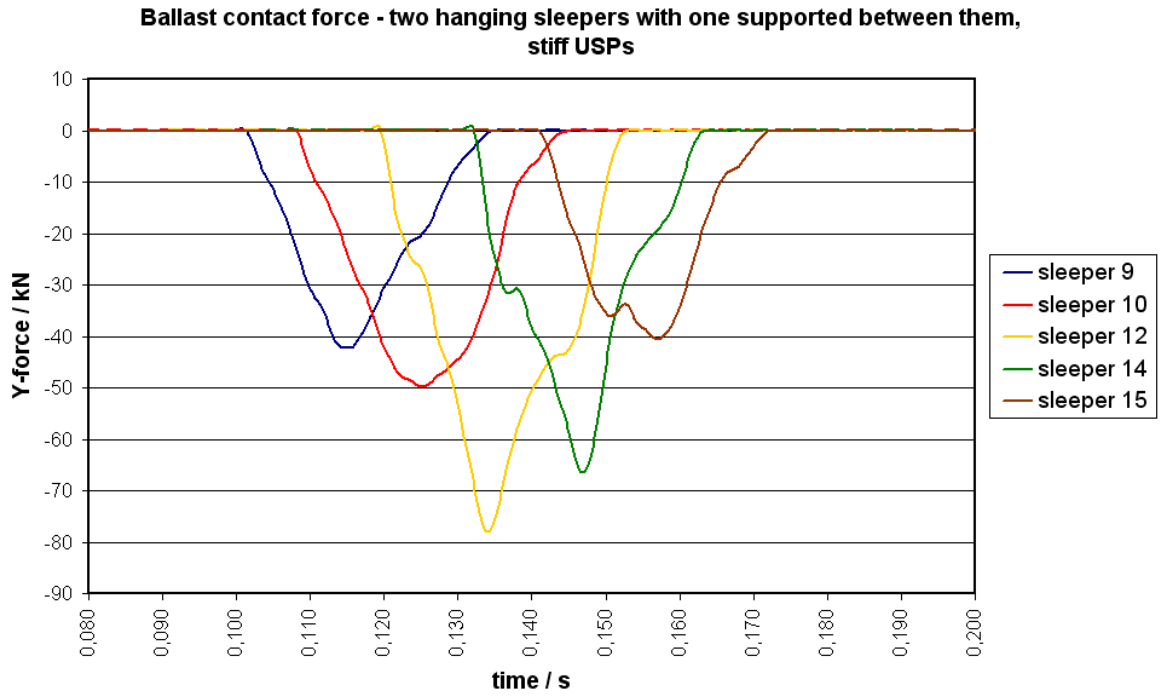

Figure 9.13: Ballast contact force with two hanging sleepers and stiff USPs

As in the other two cases examined the contact forces with stiff USPs (shown in Figure 9.13) look similar to the forces when using no USPs, but the forces are now slightly lower. The maximum contact force at sleeper 9 is now -42 kN and at sleeper 10 it is -50 kN. The maximum forces at sleeper 12 decreases about 2 kN to -78 kN now. At sleeper 14 the maximum contact force decreases to -66 kN. The maximum force at sleeper 15 is now -41 kN.

When using medium USPs the ballast contact forces are shown in Figure 9.14. The behaviour of the contact forces look similar to the forces in the first two cases but the forces are less peaky and have a longer duration. In front of the first hanging sleeper the maximum contact force increases from -32 kN at sleeper 9 to -36 kN at sleeper 10. The highest maximum contact force occurs at the intermediate sleeper 12 with -57 kN. After the second hanging sleeper the maximum contact forces decrease to -49 kN at sleeper 14 and to -34 kN at sleeper 15. At sleeper 15 the contact force looks again like the force at sleeper 9 in front of the hanging section.

The contact forces when using soft USPs are shown in figure 9.15. The maximum

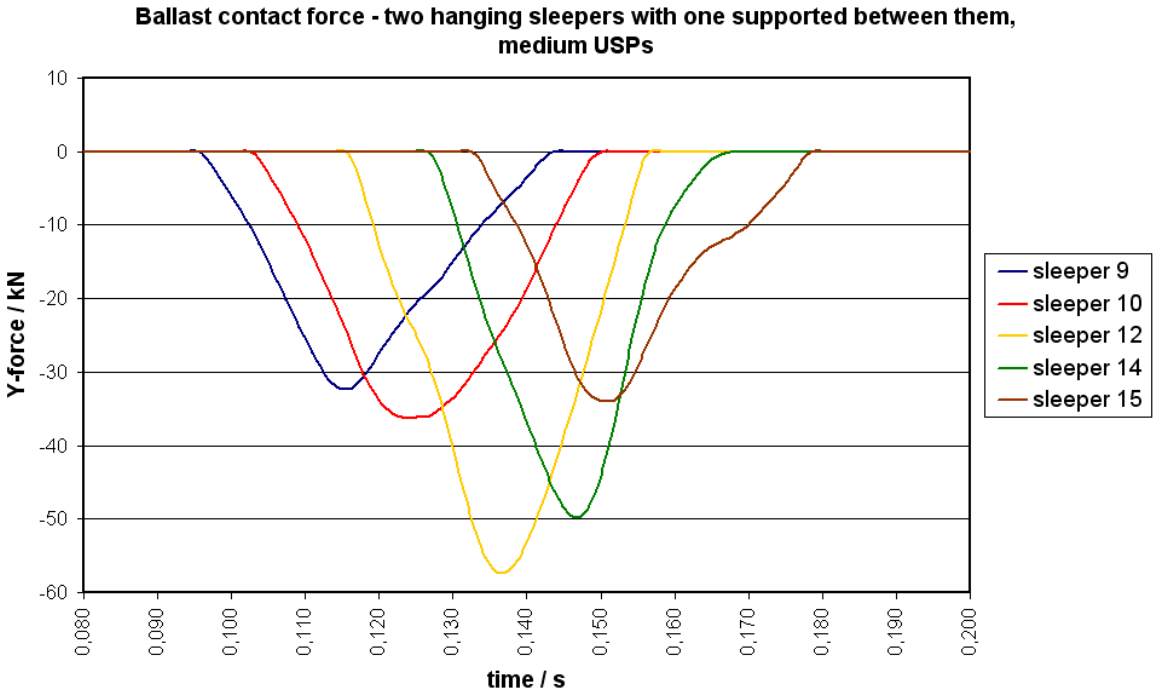

Figure 9.14: Ballast contact force with two hanging sleepers and medium USPs

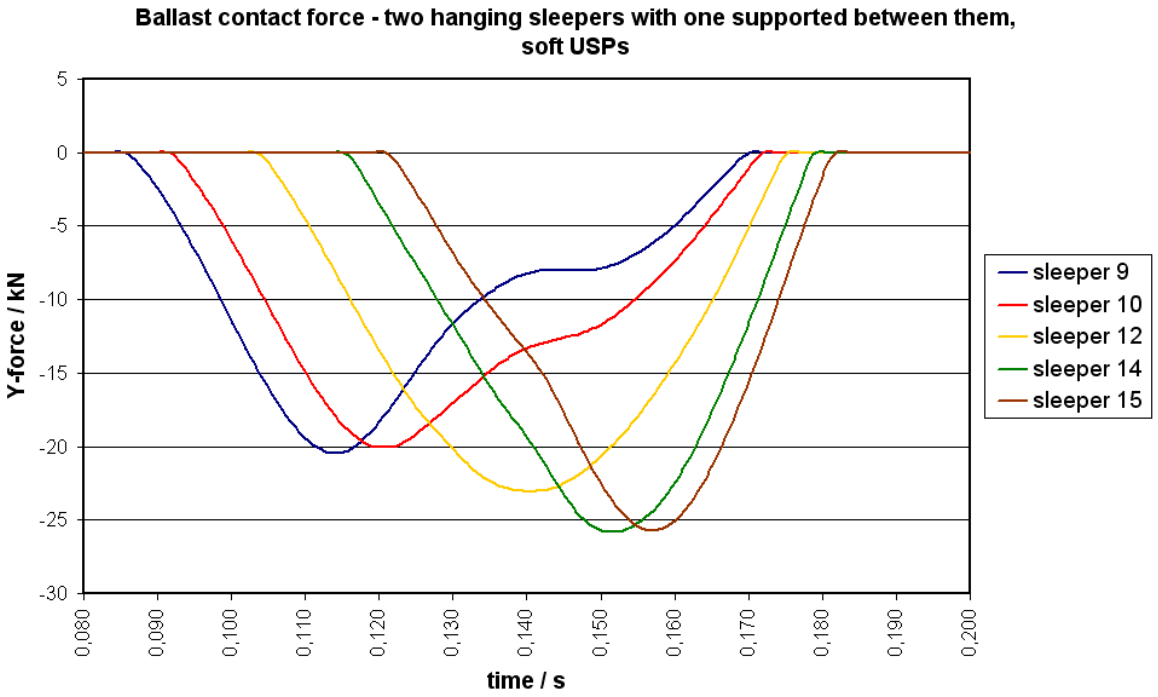

Figure 9.15: Ballast contact force with two hanging sleepers and soft USPs

contact force in front of the first hanging sleeper is -20 kN both at sleeper 9 and at sleeper 10. At sleeper 12 the maximum contact force is -23 kN. At sleeper 14 the maximum contact force becomes -26 kN and it reaches the same maximum value also at sleeper 15. Noticeable is that the force in this case is higher after the second hanging sleeper than at the sleeper between the two hanging sleepers.

USPs	**no**	**stiff**	**medium**	**soft**
sleeper 9	-46 kN	-42 kN	-32 kN	-20 kN
sleeper 10	-52 kN	-50 kN	-36 kN	-20 kN
sleeper 12	-80 kN	-78 kN	-57 kN	-23 kN
sleeper 14	-72 kN	-66 kN	-49 kN	-26 kN
sleeper 15	-51 kN	-41 kN	-34 kN	-26 kN

Table 9.3: Maximum ballast contact forces with two hanging sleepers and one supported sleeper between them

Table 9.3 shows all the received maximum ballast contact forces for the case of one supported sleeper between two hanging sleepers.

9.4 Results

By using stiff USPs there are only small differences in the wheel/rail contact forces compared to not using any USPs at all. The hanging sections cause high peaks of the wheel/rail contact forces. It is remakable that in the cases of one hanging sleeper and three adjacent hanging sleepers the peak load gets a little bit higher with the use of stiff USPs compared to using no USPs. But with a supported sleeper between two hanging sleepers the load peaks get a little bit smaller when stiff USPs are used. After the hanging sections the wheel/rail contact forces oscillate with higher amplitudes in the case of using no and stiff USPs. With the use of medium USPs the peaks of the wheel/rail contact forces are smaller in all cases examined. But the forces oscillates with much higher amplitudes and time periods after the wheel has passed the hanging section.

The influence of softer USPs on the ballast contact forces is immense. When using softer USPs the maximum ballast contact forces on the sleepers next to the hanging ones decrease. But in all cases examined there is no difference in the contact force at the sleeper which is located two sleepers before the first hanging one. All maximum contact forces are the same in all cases examined. So one can conclude that a sleeper

two sleepers and more before a hanging sleeper does not get affected by the hanging sleepers. Behind the hanging sections more sleepers are affected by the hanging ones. The maximum forces at the sleeper located at the second section after the last hanging sleeper may vary a lot. The maximum force at this sleeper can become very low but also higher than the maximum force in front of the hanging sections. Also the times of loading of the sleeper located in front of the hanging sections becomes longer. When using softer USPs these times loading become longer. With medium and soft USPs they often continue until the wheel has left the hanging sections. When using no, stiff and medium USPs the maximum contact forces occur at the first sleeper after the hanging sections in the case of one and three hanging sleepers. In the case of one supported sleeper between two hanging sleepers the intermediate sleeper carries the highest forces. In all cases the maximum contact forces at the highest sleepers loaded decreases about 50% when using medium USPs compared to using no USPs. When using stiff USPs these changes are only small. With using soft USPs the variations of the contact forces between all examined cases are very small.

10 Summary and conclusions

In this work the influence of USPs on the wheel/rail contact force and on the ballast contact forces is examined. Three different types of USPs (see Table 7.1 on page 16) are used in this work: stiff, medium and soft ones. The three types of USPs used have different Young's moduli in order to get different stiffnesses. The results obtained when using these types of USPs are compared to the results when using no USPs.

Three different cases are studied in this work. The first case studied in Chapter 7 is a transition from a soft part of the track to a stiffer part. In Chapter 8 the influence of a randomly varying track stiffness on the contact forces is examined. The last case, examined in Chapter 9, are hanging sleepers. Three different cases of hanging sleepers are examined: one hanging sleeper, three adjacent hanging sleepers and two hanging sleepers with one supported sleeper between them.

The USPs will influence the wheel/rail contact forces. The differences when using stiff USPs compared to using no USPs are small. At a transition area the load peaks do not differ. The differences on the random track are also small. The maximum ranges differs by about 4 kN only and the calculated load spectra are similar to using no USPs. Remarkable is that the load peaks caused by hanging sleepers may even increase with using stiff USPs as compared to using no USPs. A reason for these small changes of the wheel/rail contact forces may be that the stiff USPs are too stiff. Thus, they do not influence the total vertical stiffness of the track very much.

When using soft USPs there is no influence of the ballast stiffness on the wheel/rail contact forces any longer. The two received forces when using soft USPs on the transition area and on the random track look almost the same and there are no big differences in the load spectra achieved at the two examinations. Compared to the other examinations higher ranges occur and the period times increase. It seems that the USPs are too soft. By using them the whole track becomes very soft and there is no influence of the ballast on the total track stiffness any longer.

The best results for the wheel/rail contact forces are achieved when using medium stiffness USPs. With this type of USPs the smallest variations of the contact force

occur on a random track and the peak caused by a transition disappears. Also the maximum force ranges caused by hanging sleepers are smaller when medium stiffnes USPs are used. But after the hanging sections and transitions the wheel/rail contact forces oscillate with higher ranges. Nevertheless the maximums ranges becomes the smallest of all cases examined.

The USPs also influence the ballast contact force. When using softer USPs the maximum contact forces decrease. Simultaneously the loading times become longer when softer USPs are used. This shows that the load from the passing trains are distributed over more sleepers. As a result of these effects the damage to the ballast is reduced and a longer lifetime can be expected.

Summing up all these aspects one can see that USPs may have a positive effect on the train/track interaction forces. But the stiffness of the USPs must be carefully chosen in order to achieve good results.

11 Bibliography

[1] Berggren, E.: Dynamic Track Stiffness Measurement - A New Tool for Condition Monitoring of Track Substructure. Licentiate Thesis, Railway Technology, Royal Institute of Technology, Stockholm, Sweden, 2005;

[2] Dahlberg, T.: Track Issues. In: Iwnicki, S. (editor): Handbook of railway dynamics, CRC Press, London, 2006;

[3] Friederich, K.: Einfluss der Bauwerk-Baugrund-Wechselwirkung auf das dynamische Verhalten des Eisenbahnoberbaus. Dissertation, Fakultät für Bauingenieurwesen, Ruhr-Universität Bochum, Bochum, Germany, 2004;

[4] Haibach, E.: Betriebsfestigkeit - Verfahren und Daten zur Bauteilberechnung, 3. Auflage, Springer Verlag, Berlin, Germany, 2005;

[5] Hallquist, J. O.: LS-DYNA - Theory Manual. Livermore Software Cooperation, Livermore, California, United States of America, 2005;

[6] Holtzendorff, K.: Untersuchung des Setzungsverhaltens von Bahnschotter und der Hohllagenentwicklung auf Schotterfahrbahnen. Dissertation, Fakultät V - Verkehrs- und Maschinensysteme, Technische Universität Berlin, Berlin, Germany, 2003;

[7] Ilias, H.: Nichtlineare Wechselwirkungen von Radsatz und Gleis beim Überrollen von Profilstörungen. Dissertation, VDI-Verlag, Berlin, Germany, 1996;

[8] Johansson, A.: Under Sleeper Pads - Influence on Dynamic Train-Track Interaction. Research report 2006:02, Department of Applied Mechanics, Chalmers University of Technology, Gothenburg, Sweden, 2006;

[9] Knothe, K. and Y. Wu: Receptance behaviour of railway track and subgrade. In: Archive of Applied Mechanics, Volume 68, Numbers 7-8, pp 457-470, August 1998;

[10] Lalanne, C.: Mechanical Vibration & Shock, Volume IV: Fatigue Damage. Hermes Penton Service, London, 2002;

[11] Leykauf, G. and W. Stahl: Tests and experiences with sleeper pads. In: EI - Eisenbahningenieur (55), booklet 6, pp 8-16, 2004;

[12] López Pita, A., P. F. Teixeira and F. Robuste: High speed and track deterioration: the role of vertical stiffness of the track. In: Proceedings of the Institution of Mechanical Engineers, Part F, Volume 218, pp 31-40, Number 1/2004;

[13] Lundqvist, A.: Dynamic train/track interaction - Hanging sleepers, track stiffness variations and track settlement. Licentiate thesis, Thesis No. 1159, Division of Solid Mechanics, Department of Mechanical Engineering, Institute of Technology, Linköping University, Linköping, Sweden, 2005;

[14] Lundqvist, A., R. Larsson and T. Dahlberg: Influence of railway track stiffness variations on wheel/rail contact force. Proceedings "Track for High-Speed Railways", pp 67-78, Porto, Portugal, October 2006;

[15] Nielsen, J.C.O.: Train/Track Interaction - Coupling of Moving and Stationary Dynamic Systems - Theoretical and Experimental Analysis of Railway Structures Considering Wheel and Track Imperfections. PhD thesis, Department of Solid Mechanics, Chalmers University of Technology, Gothenburg, Sweden, 1993;

[16] Popp, K., H. Kruse and I. Kaiser: Vehicle-Track Dynamics in the Mid-Frequency Range. In: Vehicle System Dynamics, Volume 31, pp 423-464, 1999;

[17] Remennikov, A. and S. Kaewunruen: Experimental investigation on dynamic railway sleeper/ballast interaction. In: Experimental Mechanics, Volume 46, Number 1, pp 57-66, February 2006;

[18] Riessberger, A.: Ballast track for high speeds. Proceedings "Tracks for High-Speed Railways", pp 23-44, Porto, Portugal, October 2006;